Developments in Heat and Water Balance Coupling for Micro-Climate Modelling of Urban Squares under the Influence of Greening – A Review and Case Study

Clara Zeh

2023

TU Delft

MSc Thesis in Civil Engineering Track Water Management

Developments in Heat and Water Balance Coupling for Micro-Climate Modelling of Urban Squares under the Influence of Greening - A Review and Case Study

Clara Zeh

October 2023

A thesis submitted to the Delft University of Technology in partial fulfillment of the requirements for the degree of Master of Science in Civil Engineering track Water Management

Supervision: Dr.ir. Martine Rutten
Dr.ir. Miriam Coenders
MSc Eva Stache

Abstract

Urban areas are prone to extremely high temperatures as a result of climate change and the urban heat island effect. Urban micro-climate modelling has become an important tool to evaluate the effect of heat mitigating measures and develop climate-sensitive urban designs. However, many models lack the accurate fine scale simulation of evapotranspiration influence and soil moisture conditions to predict human thermal comfort (HTC).
This works objective is to better understand the coupling of the heat and water balance for micro-climate predictions of urban squares and its influence on the HTC, especially under the influence of greening. Therefore, a literature review on recent model developments was conducted. Additionally, a case study was performed for the Heat Square in the Green Village using the model VTUF-3D, chosen based on the literature review.
Five urban micro-climate models work on the fine scale water balance representation, namely ENVI-met, i-Tree Hydro+, Solene-Microclimat, ST, and VTUF-3D. ENVI-met offers comprehensive analysis options of greening solutions and user-friendliness, while VTUF-3D excels in detailing soil and plant characteristics. Given the detailed water balance simulation and the accurate trend prediction for the latent heat flux, it is expected that greening effects on the urban micro-climate of the Heat Square can be predicted accurately with VTUF-3D, if not for spatial and human thermal comfort assessment.
The reviewed models require further model development towards a comprehensive water balance representation and related greening analysis options. Additionally, further efforts towards model applicability are needed, including validation and user-friendliness. VTUF-3D requires improvement of spatial variability representation and HTC prediction.
Note, the literature review is no holistic assessment and does not provide a conclusion on the overall performance of the models. The case study was limited in model feature configuration.

Acknowledgements

First and foremost, I would like to express my heartfelt gratitude to Dr.ir. Martine Rutten for her invaluable guidance and unwavering support throughout my research journey, always attuned to my individual needs.

I extend my sincere thanks to Dr.ir. Miriam Coenders and Eva Stache for their priceless feedback and insightful suggestions, which provided me with fresh perspectives on my thesis.

I offer my special appreciation to Dr. Kerry Nice and Dr. Ronald van Nooyen for their generous assistance in setting up and configuring VTUF-3D. I would like to extend my sincere thanks to the Green Village team for their invaluable help in data collection on the Heat Square.

My friends have been a tremendous source of moral support and encouragement throughout my thesis, and I wish to extend my gratitude to them. I am particularly thankful to my housemates, who warmly welcomed me to the Netherlands and provided essential moral support, especially during the challenging times of the COVID-19 pandemic.

I am deeply thankful to Tjark for his continuous support and meticulous review of my report. Having you by my side brings me great happiness.

Last but certainly not least, I would like to express my profound appreciation to my parents for their love and unwavering support.

Contents

List of Figures

List of Tables

Acronyms

Cfb	temperate oceanic climate
CFD	computational fluid dynamics
COV	coefficient of variation
HTC	Human Thermal Comfort
PMV	Predicted Mean Vote
SEB	Surface Energy Balance
SPA	soil plant atmosphere
SWB	Surface Water Balance
UTCI	Universal Thermal Climate Index

$LW_{up,m}$	Upwelling longwave radiation modelled, square average
$LW_{up-grass,m}$	Upwelling longwave radiation modelled, square average
$SW_{up,m}$	Upwelling shortwave radiation modelled, square average
$SW_{up-grass,m}$	Upwelling shortwave radiation modelled, square average
$T_{road,m}$	Road surface temperature modelled, square average
$T_{air,m}$	Canyon air temperature modelled, square average
$T_{air-grass,m}$	Canyon air temperature above grass modelled
$T_{ground,m}$	Ground surface temperature modelled, square average
$T_{soil,m}$	Soil temperature of top layer (0.1 m) for grass patch modelled
$\theta_{soil,m}$	Soil moisture modelled for grass patch

$LW_{up-pav,o}$	Upwelling longwave radiation measured above traditional pavement
$LW_{up-con,o}$	Upwelling longwave radiation measured above concrete
$LW_{up-grass,o}$	Upwelling longwave radiation measured above grass
$SW_{up-pav,o}$	Upwelling shortwave radiation measured above traditional pavement
$SW_{up-con,o}$	Upwelling shortwave radiation measured above concrete
$SW_{up-grass,o}$	Upwelling shortwave radiation measured above grass
$T_{con,o}$	Concrete surface temperature measured
$T_{air-con,o}$	Canyon air temperature measured 1.4 m above concrete
$T_{pav,o}$	Traditional pavement surface temperature measured
$T_{air-pav,o}$	Canyon air temperature measured above traditional pavement
$T_{sfc-soil,o}$	Soil surface temperature measured on grass patch
$T_{air-grass,o}$	Canyon air temperature measured above grass
$\theta_{soil,o}$	Soil moisture measured at -8 cm for grass patch

1 Introduction

Urban areas are prone to extremely high temperatures as a result of climate change and the urban heat island effect. Urban micro-climate models are used to create climate-sensitive urban designs, but many models lack the accurate fine scale simulation of evapotranspiration influence and soil moisture conditions to predict human thermal comfort.

The introduction provides background information on the importance of climate sensitive urban design (1.1). Section 1.2 introduces the research problem and motivates the relevance of improving the understanding of the heat and water balance coupling for micro-climate predictions of urban squares. Section 1.3 states the thesis objective and research questions, followed by the thesis outline in section 1.4.

1.1 Societal Relevance of Urban Heat Mitigation

Due to climate change heatwaves become an increasing issue for the human well-being [2; 3]. Heat exposure poses a variety of serious health issues including heat stress and heat stroke, acute kidney injury, exacerbation of congestive heart failure [4], and increased risk of interpersonal [5], and collective violence [6]. The heatwave of 2003 caused about 70,000 deaths in Europe [7]. More recently, the heatwave over the summer of 2022 caused about 60,000 deaths in Europe [8]. In the future, an increased mortality due to heatwaves is expected globally [9]. Especially urban areas are prone to extremely high temperatures as a result of the urban heat island effect. High-density infrastructures block air flow, trap radiation, and emit stored heat from solar radiation and exhaust heat [10].

Consequently, urban heat mitigating measures are intensively researched to improve Human Thermal Comfort (HTC). HTC is influenced by air and mean radiant temperatures, humidity, wind, and individual factors like clothing, level of activity, age, gender, height, and weight [1]. To determine outdoor thermal comfort, the Universal Thermal Climate Index (UTCI) is a commonly used indicator [11]. Other indicators include the Predicted Mean Vote (PMV), Gagge's ET*, and SET* [12]. The mean radiant temperature was found to be the main driver of HTC during daytime [13] and air temperature during nighttime [14]. However, the intricate and diverse three-dimensional composition of urban areas leads to significant spatial and temporal variability of the environmental factors [15]. Hence, for HTC assessment it must be looked at the micro-climate, which is the dominant climate at the micro-scale, arising form the diversity found within the urban canopy layer modifying local climate factors [16]. The micro-scale can vary depending on the level of heterogeneity [16], starting at a few meters. In the urban area it is useful to look at the square scale to represent this heterogeneity [16; 1]

Urban heat depends on the urban characteristics, such as material properties, object arrangements and shapes, as well as vegetation and soil properties. Hence, HTC can be promoted by improving the urban characteristics, e.g.by increasing the albedo, providing shade, or promoting air flow. Especially greening is a prominent suggestion [17; 18]. Its cooling effect via evapotranspiration and shading has been confirmed in observational studies [19]. In particular, it is suggested to increase the number of urban trees in order to enhance the cooling effect [20]. Urban greening increases liveability and addresses environmental challenges caused by urbanization with additional ecosystem services such as gaseous pollutant uptake [21], storm water retention [22], improved biodiversity [23], cultural, aesthetic, and health benefits [24; 25]. However, the cooling effect of greening is strongly dependent on plant dimensions and plant physiological characteristics, that are vegetation species specific parameters determining plant functioning and

transpiration beyond structural characteristics [26; 27]. A limiting factor for the cooling potential of urban greening is the soil water availability [21]. The soil water availability is dependent on water input, including precipitation, irrigation, and water pipe leaking, as well as soil type characteristics [12]. Climate change promotes the frequency and intensity of droughts and floods globally [28]. Again, urban areas are especially prone to these extreme events. Impervious surfaces, exploitation of groundwater, building material and configurations, and anthropogenic exhaust heat and aerosols have altered the urban water cycle and impacted water sustainability [29]. Impervious surfaces disable infiltration and groundwater recharge, while urban heat and aerosols influence precipitation [30]. Urban drought impacts the inhabitants health and the cities economy, decreasing the life quality in urban areas [29]. Many cities have yet to achieve resilience to drought, which is correlating with heat waves [29]. While drought is a limiting factor for plant transpiration and the cooling potential of urban greening, greening can also help store water during wet seasons and release it during dry periods, improving urban water sustainability [29].

Urban micro-climate modelling has become an important tool to evaluate the above introduced heat mitigating measures and configurations on their HTC effects for an urban area [31]. This way climate-sensitive urban designs can be developed.

1.2 Scientific Relevance of Urban Micro-Climate Modelling

To predict HTC effects, an understanding of the urban Surface Energy Balance (SEB) and Surface Water Balance (SWB) is required, as illustrated in Figure 1.1. The SEB provides a statement of energy conservation to assess thermal energy (heat) transfer and storage in an urban system and its interaction with the atmosphere. It can be set up for the characteristics of individual urban features or a whole system. The SEB can be written as [1]:

$$Q* + Q_F = Q_G + Q_H + Q_E + \Delta Q_S + \Delta A \tag{1.1}$$

with $Q*$ being the net radiation for short (solar) and longwave (terrestrial) radiation, and Q_F the anthropogenic heat flux introduced from human activities (living, work, travel). Q_G describes the ground heat flux - sensible heat transfer to a substrate by conduction. Q_H is the sensible heat flux, describing the heat transfer from a surface to the atmosphere by convection, warming the lower atmosphere. Q_H is driven by temperature differences. Q_E, the latent heat flux, also describes energy transfer from a surface to the atmosphere. However, in form of water vapour. Latent heat refers to the energy used to vaporize the water, removing energy from the local environment, and causing the surface and near-surface air to cool, while adding humidity [1]. ΔQ_S is the net heat storage change, and ΔA the net energy change though advection (air flow).
The SWB is powered by the SEB, through evapotranspiration, convection, advection, and condensation restocking water stores, like soil moisture. It describes the partitioning of available water. The SWB accounts for all water passing through or stored in a defined urban area (volume). The SWB for an urban square can be written as [1]:

$$P + I + F = \delta R + E + \delta S + G + \delta A \tag{1.2}$$

with input terms P describing precipitation, I being the piped water imported to the area, and F being the water formed chemically by fuel combustion in air. δR is the net runoff of surface water, δS the change in storage including soil water, groundwater and any surface water stores like interception and ponding, and δA the atmospheric storage change through advection. G describes the groundwater. Evapotranspiration (E), links the SWB and SEB through conversion to latent heat by the latent heat of vaporization.

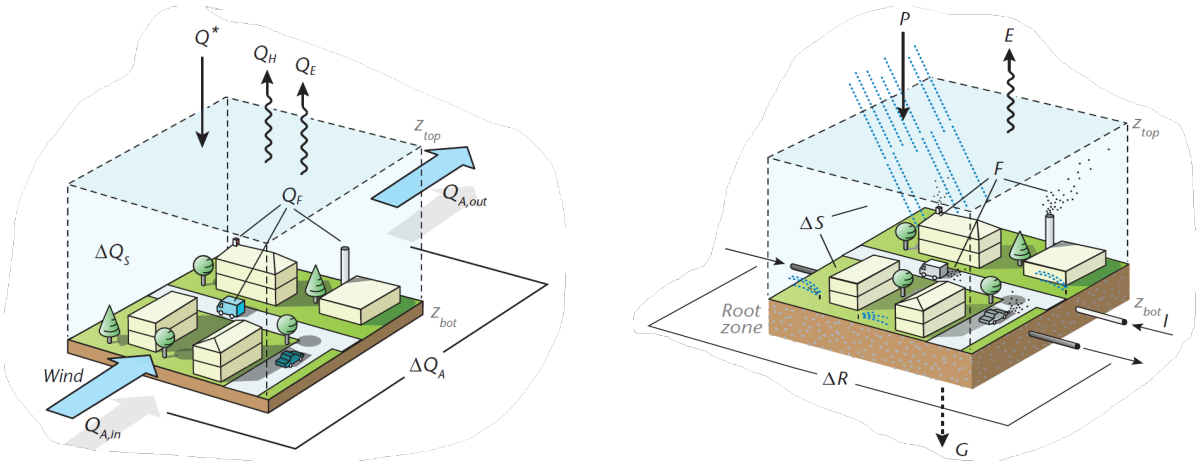

(a) SEB (b) SWB

Figure 1.1: The urban surface energy balance (SEB) and surface water balance (SWB) [1].

To make reliable predictions for the effect of heat mitigation strategies and configurations it is important that all climate influencing factors and underlying processes are represented well in an urban micro-climate model.
Simulating urban climate can be distinguished into four coupled categorise that are part of the SEB and SWB: radiation, air flow, thermodynamics, and hydrology [32]. Radiation accounts for solar (short wave) and terrestrial (long wave) radiation and its interaction with the urban form and atmosphere through reflection, transmission, and absorption - resulting in heating and cooling of the respective medium [1]. Hence, incoming radiation, material properties, and object arrangement need to be considered to represent the influence of radiation on urban climate [1]. Air flow accounts for wind speed and direction, and convective exchanges transporting heat [32]. Therefore, the consideration of object arrangement, shape, roughness, and thermal energy is important to consider [1]. Thermodynamics describe the available energy in form of heat [33]. Therefore, heat conduction and storage in urban surfaces must be simulated for urban climate prediction [32]. The fourth part is hydrology capturing and converting energy through evapotranspiration to latent heat [1]. Therefore, the parameters of the SWB must be considered, which are dependent on surface cover, soil and vegetation properties.
However, the cooling potential of urban greening is commonly evaluated solely for tree shading, because of the complexity of resolving all vegetation-urban climate interactions at larger scales [34]. The models are typically computationally demanding, difficult to parameterize and sensitive to boundary conditions [21]. This goes for simulation approaches based on computational fluid dynamics, urban canopy models, and large-eddy simulation approaches [21]. Therefore, the consideration of vegetation species and individual plant properties is limited [21]. Additionally, many urban tree models are missing to model soil water availability, or have not been assessed sufficiently [21]. This limits the models value as decision support tool for climate-sensitive urban designs [21].

This assessment is supported by a review paper from 2021 [27]. Its considered 130 peer-reviewed papers on 21 urban micro-climate models, published between 2006 and 2019 [27]. The review found that many models focus on micro-climate simulations based on radiation, airflow, and thermodynamics, also when it comes to the cooling effect of vegetation. It was found that "many studies have examined the cooling effect of vegetation on solar radiation and wind speed" with a focus on accurate vegetation parameterisation and fine scale simulations [27]. The review highlights contrasting cooling effects of vegetation found in several studies [34; 35] and points out that the tree shade effect is dependent on sufficient water supply [36; 27]. The review suggests further studies enhancing the methods for modelling soil moisture conditions and evaporative cooling [27]. The review leaves room for the assessment of models which have not been covered, that is recent model developments (which have not been peer reviewed).

1.3 Objectives and Research Questions

The purpose of this research is to address the lack of accurate fine scale modelling of evapotranspiration influence and soil moisture conditions to accurately predict the urban micro-climate and human thermal comfort. The objective is to better understand the coupling of the heat and water balance for micro-climate predictions of urban squares and its influence on the human thermal comfort, especially under the influence of vegetation.

Main Research Question:
How well can recent developments in urban micro-climate modelling predict the influence of greening on the micro-climate of urban squares?

Sub-questions:

1. How is the coupled heat and water balance described in recent model developments?
2. What is the applicability of the recent model developments?
3. How does the human thermal comfort develop through heat mitigation via greening, considering the coupled heat and water balance in simulations for an urban square in the Netherlands?

1.4 Thesis Outline

This section outlines how the research question is addressed and provides an overview of the thesis structure. To develop a better understanding of the coupled heat and water balance for urban micro-climate predictions this investigation starts with a literature review in Chapter 2. The literature review aims to answer the research sub-questions one and two. An overview and assessment of urban micro-climate simulation studies integrating soil water availability and plant physiological characteristics in the models is provided. Note, the literature review is no holistic assessment of the model capabilities but focuses on the integration of the water balance.
Based on the literature review the VTUF-3D model is selected to assess the human thermal comfort development of the Heat Square in the Green Village, Delft and to provide further model assessment. Here the aim is to answer the research sub-question three and extend the answer to sub-question two. The Heat Square is a small urban square on which heat mitigation measures are being assessed via several meteorological measurements. Data for different square configurations exists providing the basis for the case study. Chapter 3 contains the methodology of the case study. The results and discussion of the case study can be found in Chapter 4. Lastly, Chapter 5 provides conclusions and offers recommendations for further research.

2 Literature Review on Heat and Water Balance Coupling Advances in Urban Micro-Climate Modelling

This literature review aims to provide an overview and assessment of urban micro-climate models that couple the SEB with the SWB. It seeks to highlight model capabilities and gaps for future research and urban planning. The review forms the basis for the model selection in the following case study.
Square scale models specifically assessing and representing nature-based heat mitigation strategies were evaluated for completeness and level of detail in the water balance representation. This study only includes models that describe transpiration. Transpiration is considered most important for evaporative cooling [37], [20]. In turn, the energy balance description is only roughly assessed.

Section 2.1 provides the methodology for the literature review. Section 2.2 establishes the assessment requirements. Section 2.3 contains the model analysis and assessment. A concluding summary of model capabilities and gaps for future research is provided in Section 2.4.

2.1 Model Selection and Analysis Criteria

In this section, the selection criteria for the urban micro-climate models found in literature are discussed. Additionally, the model analysis criteria, for the model overview and assessment, are established.

2.1.1 Model Selection Criteria

The model selection from literature is passively dependent on the literature search strategy. Consulted literature was limited to journal articles with academic publication settings and software package websites of established urban micro-climate models. Furthermore, only literature available in English was consulted. Google scholar was used as the main literature search engine and contact to researchers was used for up-to-date knowledge on model availability and model handling. The literature search filter included publications after 2017 only and search words and phrases as listed below.

- Fine/square/micro scale
- Urban microclimate/ heat mitigation
- Models/ simulation/ prediction
- Energy/heat/radiation and water balance coupling/integration/combination
- Evaporative cooling/ transpiration/ evapotranspiration
- Vegetation, etc.

The model selection followed four inclusion criteria. First, the water balance must be represented by the model at least to the extent of plant transpiration and soil water availability as this is the previously identified research gap to be investigated. Second, considering the level of heterogeneity of urban structures and meteorological influences, as well as soil and vegetation characteristics the selected models must be able to simulate at square scale [1]. Third, as urban micro-climate models target to aid climate sensitive urban planning the selected models must work with the real morphology of the urban area, and the analysis of nature-based heat mitigation strategies must be possible. Finally, only literature published after 2017 is used for model selection. A review from 2021 discussed 130 peer-reviewed papers on urban micro-climate

models published between 2006 and 2019 and concluded the here investigated research gap [27]. The review contained just one micro-climate model – VTUF-3D, published in 2018 – fitting the selection criteria [27]. Hence, models and model versions developed in 2018 and later are considered in this review.

Models were excluded when the water balance representation did not include plant transpiration. Also, models that do not consider plant physiological characteristics were excluded. Evaporative cooling through transpiration is a major heat mitigation strategy that needs more investigation and depends on plant physiological characteristics and soil moisture. Therefore, these factors are crucial to be included in the water balance representation [27].

2.1.2 Model Analysis Criteria

The model analysis and assessment criteria can be grouped into three categories: (1) water balance simulation approach, (2) model capabilities, and (3) model applicability.
First, the category "water balance simulation approach" aids to assess the models on a conceptual level, the completeness of micro-climate influences representation. Hence, the analysis criteria include the simulation approach and the water balance components representation.
Second, the "model capabilities" aim to indicate the possible heat mitigation strategy analysis variety and the analysis detail provided by the models. Hence, they refer to the models heat mitigation strategy analysis options, target values, applicable scale, and resolution.
Third, with the "model applicability", the model's suitability for application to urban local climate zones, and their performance is analysed and assessed. This requires criteria of number of applications - state of validation/development, tested climate, tested urban characteristics, and quality of performance including result accuracy and user-friendliness.

The focus of this study lies on the completeness of the water balance integration, the variety of the model's analysis options regarding heat mitigation strategies, and the model performance. The analysis and assessment aim to provide research opportunities to further develop the presented urban micro-climate models towards more reliable and detailed climate predictions. Radiation, thermodynamics, and air flow related influences on urban micro-climate and their representation in the related models have only been analysed and assessed conceptually, due to the scope of this report and the advanced development state of their representation in urban micro-climate modelling [27].

2.2 Analysis Criteria Requirements

This section aims to discuss the requirements of each analysis criteria for the model assessment. First, the general theory and beneficial simulation approaches for urban micro-climate modelling are summarized. Second, the water balance components and their representation with focus on soil moisture and transpiration are described. Third, the range of model capabilities is introduced. Finally, the requirements for the model applicability are discussed.

2.2.1 Simulation Approach Requirements

Various simulation approaches for urban micro-climate prediction exist. These focus on diferent climate forming categories and have certain benefits and drawbacks which are elaborated on subsequently. First, the complexity and computation time of models decreases from 3D to horizontal layering and bulk simulation [1]. The detail of 3D modelling output is high, but is also computationally demanding and usually not needed nor useful as it requires detailed and accurate parameterisation of the environment [1]. On the other hand the bulk approach does not consider internal details of the system [1].

Climate forming categories can be distinguished into four categories: radiation, air flow, thermodynamics, and hydrology. These factors influence the SEB and SWB as described in Chapter 1. Dependent on

the simulation approach, urban micro-climate models can represent the individual categories and their parameters more accurately then others.
The models considered here, can be differentiated between physical-based and process-based models, which differ in approach and level of detail. Physical-based models rely on fundamental physical laws and principles, such as conservation of mass, energy, and momentum [38]. Process-based models additionally incorporate knowledge about specific processes in a particular system [38]. Mechanistic models add a layer of detail. They attempt to describe the behaviour of a system with a detailed description of physical and chemical processes for component-based models. This includes information about structure and properties of the interconnected components [38].
Computational fluid dynamics (CFD) models are physical-based and are useful for studying fluid dynamics, heat transfer, and combustion [31]. CFD models simulate airflow and temperature fields with a high spatial resolution but also have a high computational demand [39]. Additionally, CFD models are considered black boxes, as they typically hide some assumptions and formulas from users [40].
SEB and soil plant atmosphere (SPA) models are process-based and mechanistic, depending on the level of detail. SEB models are often used to study the interactions between the land surface, atmosphere, and water cycle. They accurately capture the energy balance at the land surface, accounting for the influence of surface properties and are able to represent diurnal and seasonal variations [1]. However, they are computationally demanding and are sensitive to input data errors [41]. SPA particularly study the interactions between soil, plants, and the atmosphere.

2.2.2 Water Balance Components and Representation Requirements

The water balance integration for urban micro-climate prediction remains to be incomplete for many micro-climate models. Therefore, its aspects and description is elaborated on in this section. Additionally, considering the lack of soil moisture and plant physiological characteristics representation, the required parameterisation is discussed.

The water balance for an urban square accounts for all water passing through or is stored within the boundaries of the square over a period of time [1]. This includes the atmosphere as well as the soil volume down to the saturated soil. Figure 2.1 outlines the components of the water balance and related processes.

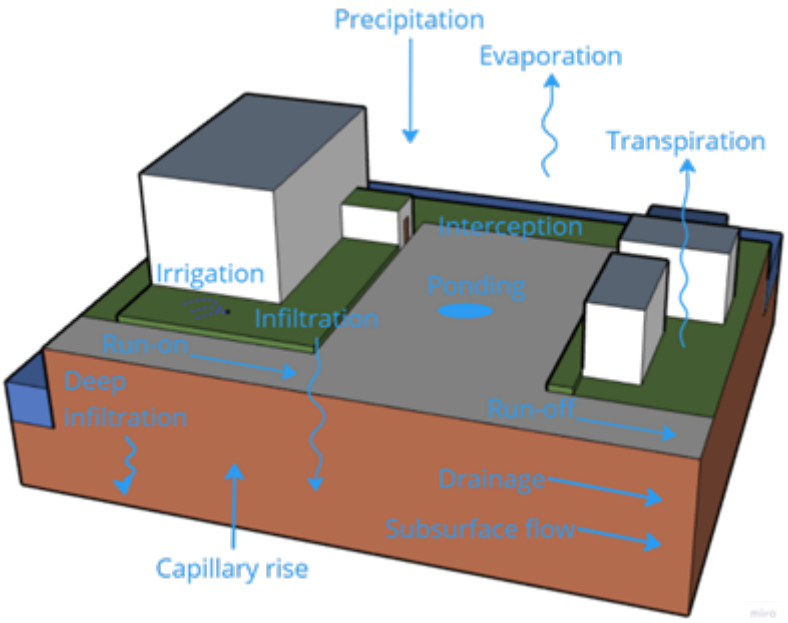

Figure 2.1: Water balance components of an urban square

The incoming water includes precipitation, run-on, irrigation, and water leakage from water pipes [1]. The incoming water is stored in the area via interception, ponding, and soil water [1].

Outgoing water comprises runoff, soil water drainage, transpiration and evaporation of open water, interception, ponding water, and soil moisture [1]. Evapotranspiration contributes to urban cooling.

Hence, these components and related processes must be represented in urban micro-climate models depending on site conditions. This takes the parameterisation of the present soil, vegetation, and ground surface characteristics to generate corresponding resistance terms for the process describing equations. Within this works scope the focus lies on the inspection of the required parameterisation of soil and vegetation as well as the representation of all water balance components. A summary of the required soil and vegetation parameterisation can be found in Table 2.1.

Soil Moisture Representation

The urban soil moisture is spatially patchy, due to the variability of the surface properties, the localized control of irrigation, and destruction of the natural soil layers through digging, pipe laying, and introduction of new materials [1]. The construction works increase hydraulic conductivity, while obstructing horizontal water movements [1]. Soil sampling is only representative at micro scale [1]. Luckily, urban squares fall into the micro scale.

Apart from the atmospheric factors precipitation, air humidity, air temperature, (solar) radiation, and wind speed, the soil water content and potential is dependent on soil water transport mechanisms like diffusion, hydrodynamic flow, capillary flow, gravity flow, evaporation, and condensation, in correspondence to the soil matrix and surface properties [42]. Additional influences are root water uptake, pipe leakage/drainage, and irrigation [1].

Describing water flow in terms of the resistance theory, the soil resistance is determined by soil matrix properties, including bulk density, grain size distribution, mineralogical and aggregate composition, besides water content and potential [42].

Transpiration Representation

Transpiration is dependent on soil moisture and vegetation species. For transpiration representation three resistance terms are required: Root resistance, xylem resistance, and water vapor transfer resistance.

The root water uptake is described by the soil resistance and root resistance for water transport [42]. The root resistance is determined by the root structure [42].

The transport within the plant can be described by the conducting vessels (xylem) resistance, impacting the root pressure and water potential in leaves [42].

The plant transpiration can then be described by the water vapor transfer resistance from the inside of the stomata chamber to the outside [42]. This determines the vapor pressure difference and the aerodynamic resistance, which in turn effects the vapor pressure difference of the leaf surface and atmosphere [42]. The aerodynamic resistance changes with wind speed, atmospheric stability over the plant cover, and the crop architecture (height and roughness) [42].

To derive the plant specific resistance terms determining transpiration, the following plant physiological traits should be known. Tree size and Leaf area index (LAI), canopy structure, xylem anatomy, wood density and root depth, water storage capacity, and stomata sensitivity to environmental drivers [43; 44; 45].

For modelling of longer time periods plant plasticity should be accounted for as well. This requires plant growth and stress physiology coupling to plant hydraulics of xylem water transport and phoem carbon transport [1]. However, the relating mechanisms remain to be unravelled [1]. As does the importance of the plant plasticity and the heterogeneity of surface and soil properties to improve the respective parameterisation needed [21].

Table 2.1: Parameterisation requirements of soil and vegetation for evaporative cooling prediction

Soil matrix parameters	**Vegetation species specific parameters**
Bulk density	Wood density
Grain size distribution	Root depth
Mineralogical and aggregate composition	Tree size
Water content	LAI
Water potential	Canopy structure
	Xylem anatomy
	Water storage capacity
	Stomata sensitivity to environmental drivers
	(Plant growth and stress physiology)

2.2.3 Model Capability Requirements

The comprehensive assessment of evaporative cooling via greening possible model analysis includes four categories: Type of greening (trees, lawn, shrubs, green walls, green roofs), vegetation species, abundance and distribution.

Depending on the detail of the analysis categories respective parameterisation is required. Evaporative cooling prediction through transpiration requires vegetation function representation. Depending on the detail of analysis this is species specific. The required parameterisation is discussed above (Table 2.1).

The main motive for urban heat mitigation is HTC and human health, respectively. Hence, the computation of HTC indices in urban climate predictions is important. Furthermore, when assessing vegetation as heat mitigation strategy, it is interesting to account for additional benefits such as air quality improvements, noise reduction, and water retention [46].

2.2.4 Model Applicability Requirements

Applicability of a model to the present conditions depends on its validation for those conditions, including climate and urban characteristics. Hence, testing for a range of conditions is important. Additionally, the models result accuracy is interesting for result assessment and further model development. Model users may also be interested in user-friendliness as performance and applicability factor. Beneficial there are a low computational demand, a comprehensive interface and operation, and easy parameterisation.

2.3 Analysis Results and Assessment of Investigated Models

Based on the previously established selection criteria a group of urban micro-climate models integrating the water balance was selected. The included models are **ENVI-met**, **i-Tree Hydro+**, **Solene-Microclimat**, **ST**, and **VTUF-3D**.

This section aims to provide an overview and assessment of the models' properties by means of the analysis criteria. The simulation approach and completeness of the water balance integration are discussed. Furthermore, focus is laid on the model capabilities and on previous model applications and their performance.

2.3.1 Water Balance Simulation Approach

Table 2.2 shows the analysis results of the relevant models. Based on the previously discussed criteria requirements, a model assessment is derived. In this category, **VTUF-3D** stands out with the most comprehensive simulation approach and water balance integration.
Concerning the modelling approach, most models apply a process-based, some even mechanistic and component-based, approach. This is beneficial for the representation of soil moisture availability and vegetation functions for evaporative cooling prediction. **ENVI-met** was found to apply the physical-based approach, describing sub-systems in less detail. Additionally, **ENVI-met** is a black box, hiding some assumptions and formulas from its users. However, **ENVI-met**, **Solene-Microclimat**, and **VTUF-3D** compute in 3D, providing results with high spatial detail. Common model gaps include offline modelling - which prevents accounting for meteorological retro-actions, and exhaust heat representation. All models lack some urban water balance components, mostly irrigation and evaporation from sealed surfaces. Note that **ST** works with soil moisture measurements instead of a simulation approach.

Table 2.2: Analysis results for simulation approach and (water balance) gaps of the investigated urban micro-climate models

Model	Featured models	Simulation approach	Water balance gaps	Additional gaps
ENVI-met	/	CFD, 3D [27]	- no evaporation from sealed surfaces [47]	- Model is a black box - Grid based portrayal of slopes & urban form complicated [32]
i-Tree Hydro+	(1) i-Tree Hydro, (2) i-Tree Cool Air	physical-based, mechanistic urban soil-vegetation-atmosphere layer scheme [48; 49]	- no irrigation - no plant growth consideration [48; 49]	- offline modelling - no wind direction [48; 49]
Solene-Microclimat	Solene (radiation), MARIE (hydrology), code Saturne (air flow)	3D, CFD coupled to radiative, thermal, and hydrological model (assumption: soil-plant-atmosphere scheme) [32]	- no irrigation - no evaporation from sealed surfaces [32]	- model coupling is touchy - no exhaust heat from cooking, vehicles [32]
ST	(1) i-Tree Eco, (2)DNDC	(1) component-based [50] (2) process-based (pollution removal) [51]	- no foliage development - no ponding & channelling - uniform soil sealing - soil moisture measured [21]	- limited to tree area [21]
VTUF-3D	(1) TUF-3D, (2) MAESPA (SPA + MAESTRA)	3D (1) SEB (2) process based soil-plant-atmosphere [52]	- no irrigation - no evaporation from sealed surfaces [52]	- offline modelling - no anthropogenic exhaust heat [52]

2.3.2 Model Capabilities

The model capabilities focus on the nature-based solution analysis options, its detail, and the target values. The analysis results are summarised in Table 2.3. As scale and resolution are model selection criteria, those are not to be further assessed. However, mind that **i-Tree Hydro+** aims at city scale, does not state a minimum scale, and is not tested at square scale. On the other hand, note that **ST** specifically looks at the energy reduction by individual trees but not at its spatial distribution.

Table 2.3: Analysis results on capabilities of the investigated urban micro-climate models

Model	Scale	Resolution	Analysis options	Parameterisation	Target values
ENVI-met	50x50 to 500x500 m [53]	0.5 m [53]	- Façade & roof greening - vegetation type - tree species - land cover type & arrangement - Water mist from fountains ENVI-met [47]	- not soil parameters but types - detailed tree geometry & leaf properties [47]	T_air; T_sfc; ET; dispersion of gases and particles; MRT, PET, UTCI [27]
i-Tree Hydro+ [48], [49]	various but aims at catchment to city scale	1 m	- UHI effects - Land cover type - Hydrology-based heat mitigation (No veg. species specification)	- soil parameters - vegetation geometry - canopy resistance	T_air; H; water quantity & quality; T_river
Solene-Microclimat [32]	street/ square/ district scale	Typ. 1 m	- Trees, roof & wall greening, lawn - Specification in grass, shrubs, perennial plants, trees	- soil type - veg. geometry	ET; T_air; T_sfc
ST [21]	Tree scale	Tree size	Drought stress effect on cooling and air pollution removal functions of trees dependent on tree species and size	- tree geometry - sap flow rate - soil moisture measurements	E_cooling; E_shading; O3 deposition velocity
VTUF-3D [52]	100x100 m, 200x200 m, (variable)	$\geq$ 1 m	Vegetation type (3 species available), abundance, distribution	- veg. geometry - veg. Species physiology (other than theory) - soil parameters	MRT; T_sfc; UTCI

ENVI-met stands out with a complete list of analysis options covering greening solutions, vegetation type and species, as well as fountain mist. The process description of the subsystems is unclear. However, it can be chosen between different soil types provided and vegetation parameterisation includes geometry and physiological traits of the leaves. They do not comply with the above developed requirements for vegetation species parameterisation though. **ST** and **VTUF-3D** stand out for their ability to explicitly assess vegetation species with its respective physiological characteristics. Note that, apart from the geometry, the models use different physiological characteristic points to describe vegetation functions.

Concerning the target values, it is interesting that only **ENVI-met** and **VTUF-3D** compute HTC indices and the vegetations effect on air quality is only assessed by **ENVI-met** and **ST**, although human health is the main driver for urban climate predictions.

Here, **ENVI-met** and **VTUF-3D** stand out for their range of analysis options, detail of parameterisation, and computation of HTC indices.

2.3.3 Model Applicability

The analysis results for model applicability are summarised in Table 2.4. Here, **ENVI-met** and **i-Tree Hydro+** stand out as commercially available models for urban planning. **Solene-Microclimat**, **ST**, and **VTUF-3D** on the other hand require further development and validation.

Table 2.4: Analysis results on applicability of the investigated urban micro-climate models

Model	Number of Applications	Climates	Study area	Urban Characteristics	Result Accuracy	User friendliness
ENVI-met	120 publicly documented applications [27]	Northern Hemisphere with Cfb [27]	Many [53]	varying	- measured & simulated long-wave radiation and relative humidity does not match [54]	commercially available [53]
i-Tree Hydro+	Assumption: multiple	Dfa	Syracuse, US	High density	- not tested for small scale & - not tested for high resolution	commercially available
Solene-Microclimat [32]	1	Cfb	Paris, France	landscaped plaza lane (assumed: high density, low-medium rise)	- requires validation with observation data	no code publicly available
ST [21]	1	Cfb exceptionally hot and dry summer	Munich, Germany	medium rise, square	- wider range of environmental conditions require testing - uncertainty in soil property initialisation - uncertainty in rainfall distribution	no code publicly available
VTUF-3D [52]	1	Cfb	Melbourne, Australia	low to medium density, open low-rise, homogeneous	- under-prediction of latent heat flux	not developed for commercial application; loose documentation

All models appear to be developed for/tested in the Northern Hemisphere mostly with temperate oceanic climate (Cfb) and require further testing. Note that all models were tested for different urban characteristics though. Only **ENVI-met** is validated for several study areas. **i-Tree Hydro+** being commercially available should be as well.

ENVI-met and **i-Tree Hydro+** are commercially available and hence expected to be most user-friendly. But considering most models apply 3D or/and process-based modelling, which is computationally demanding and requires detailed parameterisation of the environment and its subsystems, user-friendliness is relative. To what level of detail parameterization is useful, especially concerning transpiration, is yet to be investigated. **ENVI-met**, **ST** and **VTUF-3D** require a thorough parameterization of soil and vegetation, targeting the research gap while negatively affecting the user-friendliness. Note that **ST** and **Solene-Microclimat** do not have a model code publicly available. Development of result accuracy and validation for a wider range of environmental conditions is needed for all models.

2.4 Summary

The aim of this literature review was to assess existing urban micro-climate models that include the water balance to point out model capabilities and to provide an overview of gaps for future research and urban planning.

A literature study on recent model developments, referring to the coupling of the energy and water balance, was conducted. Square scale models specifically assessing and representing nature-based heat mitigation strategies were evaluated for completeness and level of detail in the water balance representation. Additionally, the general simulation approach and the applicability was evaluated. This review includes models that describe transpiration, which is considered the most important factor for evaporative cooling [37], [20]. In turn, the energy balance description was only roughly assessed.

The investigation revealed that five urban micro-climate models exist that work on the integration of the water balance, namely **ENVI-met**, **i-Tree Hydro+**, **Solene-Microclimat**, **ST**, and **VTUF-3D**. The review showed that most models apply a process-based simulation approach, beneficial for soil moisture and vegetation functions representation. However, all models lack a water balance component, mostly irrigation and evaporation from sealed surfaces. **ENVI-met**, **ST** and **VTUF-3D** stand out for their ability to explicitly assess vegetation species specific evaporative cooling effects. Interestingly, the models use different physiological parameters to describe vegetation functions. Furthermore, few models compute HTC indices. Model applicability exists for the Cfb climate but **ST**, **Solene-Microclimat**, and **VTUF-3D** require validation for a wider range of environmental conditions and are not (commercially) available. Finally, all models result accuracy require improvement.

The investigated models tackle the lack of soil moisture representation. Additionally, **ENVI-met**, **ST**, and **VTUF-3D** consider plant physiological characteristics for evaporative cooling predictions. However, the water balance representation typically misses irrigation and evaporation from sealed surfaces. Additionally, model applicability (apart from **ENVI-met**) lacks validation and user-friendliness. **ENVI-met** shows uncertainties in process descriptions though.

These findings suggest that efforts are taken to improve the coupling of SEB and SWB for the reliable assessment of nature-based heat mitigation strategies for urban planning. However, the presented models still have potential for a comprehensive water balance integration with all components, required parameterisation, and nature-based heat mitigation strategies. Additionally, the results suggest vegetation parameterisation and model applicability uncertainties.

This review is no holistic assessment of the urban micro-climate models. Whether the investigated models provide a holistic representation of the urban micro-climate is to be evaluated and potentially to be developed for. This also refers to the assessment of other heat mitigation strategies.

3 Green Village Case Study: Methodology

The goal of this case study is to explore the influence of greening on the micro-climate of an urban square in the Netherlands. To investigate this the urban micro-climate model VTUF-3D is applied to the Heat Square in the Green Village, Delft.

This chapter provides the methodology for the case study, starting by introducing the study area with the Heat Square design, the square characteristics specification and the squares meteorological measurement devices (3.1). Section 3.2 then motivates the choice for the VTUF-3D model to conduct the case study with, based on the literature review. It provides an introduction to the VTUF-3D model and describes the software requirements for the models application. Section 3.3 continues with the description of the model feature characteristics as fixed model parameters. The model input for the Heat Square simulation is described in Section 3.4, including domain and forcing data preparation. Section 3.5 concludes with the model output assessment approach.

3.1 The Study Area in the Green Village

For the case study, micro-climate simulations are performed for the Heat Square illustrated in Figure 3.1. This section describes the Heat Square design and the meteorological measurement devices on the square relevant for the simulation and its validation.

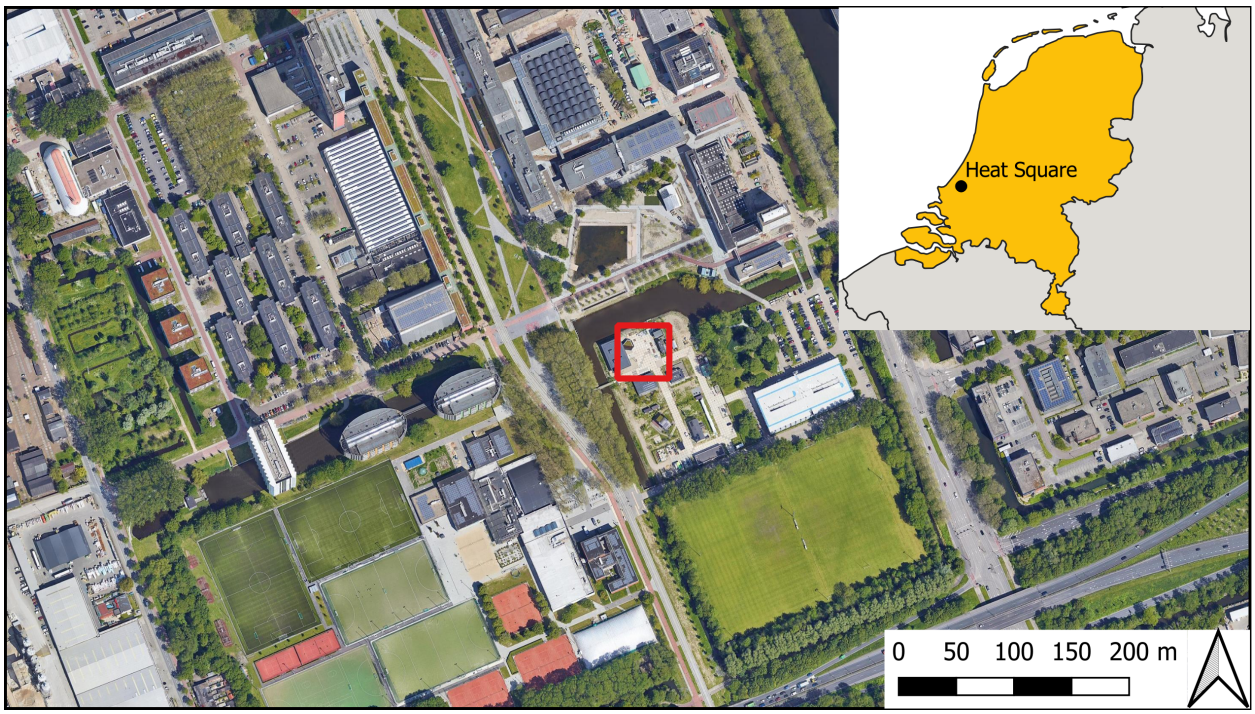

Figure 3.1: Study area location in the Green Village, TU Delft Campus, Delft, Netherlands

3.1.1 The Heat Square

The Heat Square is an urban square in the Green Village, a field laboratory for sustainable innovations in the urban area, located in Delft, the Netherlands (52°N, 4.38°E). Part of the investigations at the Green Village are focused on climate sensitive urban design. In that regard, several measurements on the urban climate are taken continuously and during field work around the Heat Square. This way changes in the square design, including heat mitigation measures are being investigated.

As illustrated in Figure 3.1, an area of 46x46 meter is investigated, which is surrounded by two water bodies, a sports complex with large outdoor soccer fields in the south-west, and large building complexes in the north-west. The close surrounding of the square has village character, with low-rise buildings and no traffic. The local climate zone (LCZ) of the Green Village is categorized as LCZ 6 DEG [36]. The climate of Delft is categorized as temperate oceanic climate (Cfb) by means of Köppen-Geiger [55].

The Heat Square is an open, rectangular, paved space. The pavement consists of 2x2 meter large concrete bricks with an extent of roughly 20x26 meter. The pavement is surrounded by shrubs and herbs in the West and North, low-rise buildings (2-5 meter high) in the West and East, and a water body in the North, see Figure 3.2a. Figure 3.3a displays a classification and the location of Heat Square features with an approximation of their height.

Since 2023, the square design changed towards more greening in the previously paved area, including patches of grass (with and without water reservoirs installed below), four red beech trees, one elm tree, and five poplar trees. Paved areas consist now of white and black vowel, as well as semi-paving with course mix (KoMex). This new design is to investigate heat mitigation and hence called 'Cool Square' from here on. A photo of the Cool Square can be found in Figure 3.2b. Figure 3.3a shows a classification and the location of Cool Square features with an approximation of their height. The detailed Cool Square design by Eva Stache can be found in Appendix A. For a detailed description of the Cool Square see [56].

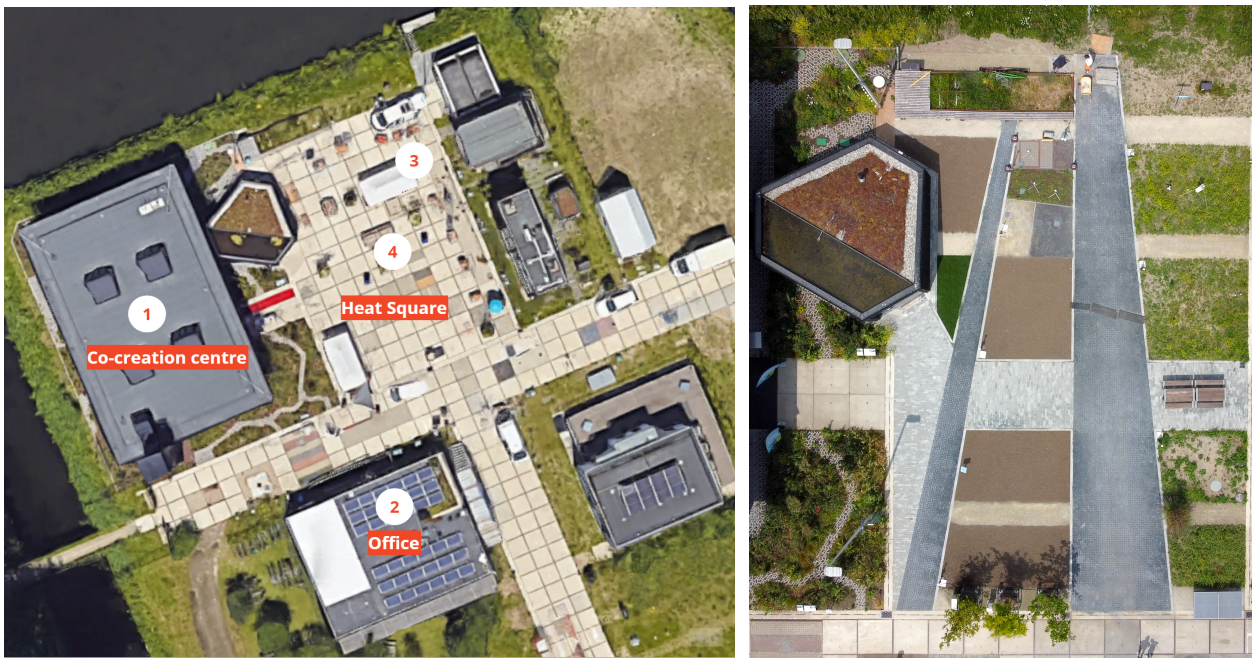

(a) Heat Square (b) Cool Square

Figure 3.2: Heat Square (a) and Cool Square (b) design and measurement locations

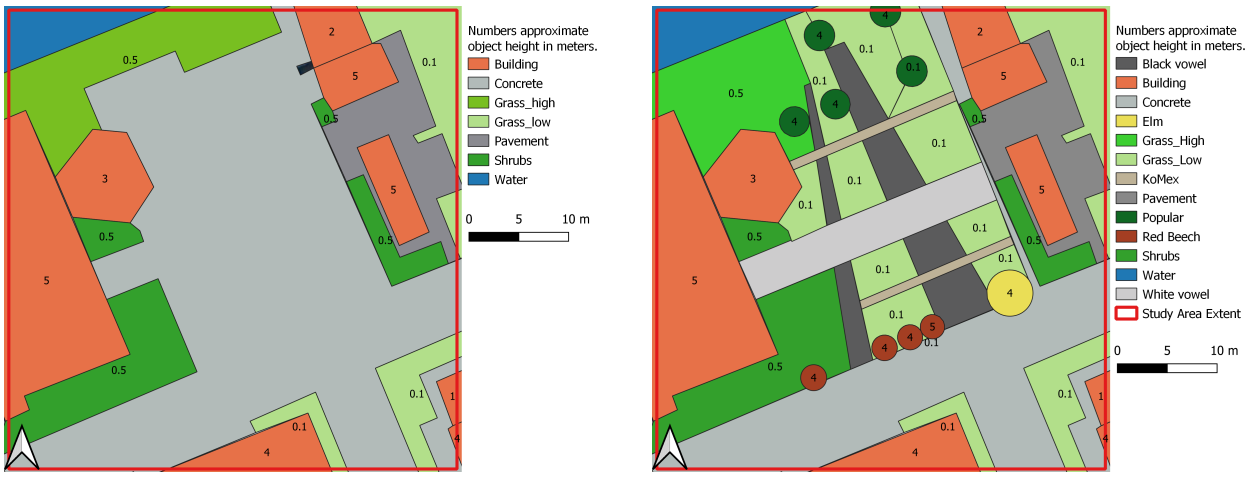

(a) Heat Square (b) Cool Square

Figure 3.3: Heat Square (a) and Cool Square (b) schematic map

Square Characteristics Specification

Here, the Heat and Cool Square characteristics are specified for surface material, soil, and vegetation species specific properties. Table 3.1 summarizes the pavement characteristics for the Heat and Cool Square. Vegetation characteristics of Elm, Poplar, and Red Beech tree are specified in Table 3.2 based on values from literature.
Soil characteristics includes Cool Square measurements for soil moisture below traditional pavement of around 0.06 m^3/m^3 and below vegetated surfaces of around 0.09 m^3/m^3 on the 13/06/2023 [56]. This data was measured with Teros 12 [56]. Soil albedo is 0.21 and soil emissivity is 0.85. These values are daytime averages measured with CR6 radiometer on 13/06/2023.

Table 3.1: Properties of structural materials on the Heat and Cool Square

Parameter	Unit	Cool Square Traditional Pavement	Source	Heat Square Concrete	Source
Albedo		0.23	daytime average measured with NR01 radiometer [56]	0.31	daytime average measured with CR6 radiometer [57]
Emissivity		0.83	daytime average measured with NR01 radiometer [56]	0.85 - 0.95	Literature [58]
Thermal Conductivity	W/mK	0.6 - 1	Literature [56]	0.5	Literature [59]
Volumetric Heat Capacity	MJ/m^3K	1.8 - 2	Literature [56]	2 - 2.8	Literature [59]

Table 3.2: Typical plant hydraulic characteristics of the trees planted on the Cool Square

Parameter	Unit	Elm (U. minor)	Red Beech (F. sylvatica)	Poplar (Populus euphratica)
Tree size	m	2.3	0.5 - 1	6
Tree age	year	1	1	
Leaf-specific xylem conductivity	$kg/(m^2\ s\ MPa)$	9.38e-5	5.48e-4	4.58e-5
Source		[60]	[61]	[62]

3.1.2 Observational Devices

Meteorological measurements taken in and around the square are employed to support and verify the climate simulations. These measurements encompass various parameters from different locations and time periods, reflecting the different square configurations. Table 3.3 summarizes the measurement devices on and around the square with measurement height, frequency, and period and refers to Figure 3.2a to locate the devices on the square. Note that the NR01 radiometer moved on the Cool Square for measurements dependent on surface characteristics [56].

Table 3.3: Specification of measurement devices around the Heat/Cool Square. See Figure 3.2a for Device location indicated by 'map location' value.

Device	Map Location	Height	Frequency	Period
Weather Station Co-creation Center	(1)	6 m	30 min	continuous
Davis Weather Station	(2)	6 m	1 h	continuous
CR6 Radiometer	(3)	1 m	1 min	18/07/22 - 06/08/22
Testo 174H	(4)	0 & 1.4 m	2 min	18/07/22 - 06/08/22
Testo 176T4	(4)	-0.14 & 0 m	2 min	18/07/22 - 06/08/22
NR01 Radiometer	(4)	1 m		05/06/23 - 18/06/23

3.2 The Model: VTUF-3D

The VTUF-3D model has been selected for the case study based on the literature review. Arguing for VTUF-3D is the models extensive plant physiological parameterisation and its assessment of the human thermal comfort via UTCI. Additionally, VTUF-3D is not a black box and requires further validation. This is in contrast to ENVI-met, which also provides a comprehensive assessment of urban micro-climate influences (see 2).

The "Vegetated temperatures of urban facets in 3D" model, VTUF-3D, is an energy balance model that allows for integration of urban greenery [52]. It is based on the urban micro-scale three-dimensional surface energy balance model TUF-3D [57]. The model categorizes surfaces as roofs, walls, and streets sub-divided in raster patches building a 3D geometry. It considers radiation, conduction, and convection, where radiation is described with the radiosity approach, accounting for numerous reflections and shading of direct solar radiation. They use finite differencing of the heat conduction equation to calculate conduction. And they describe convection by empirically relating patch heat transfer coefficients to the momentum forcing and the building morphology. TUF-3D solves radiative transport and buildings heat storage accurately [41].
For vegetation modelling the MAESPA process-based tree model [63], capable of individual tree, vegetation, and soil component modelling, is integrated into TUF-3D. MAESPA is based on the combined ecosystem models MAESTRA [64], for above-ground vegetation components simulation, and SPA [65; 66], for water balance components simulation [63]. MAESPA models "stomatal conductance, root water uptake routines, drainage, infiltration, runoff, canopy interception, as well as detailed radiation interception and leaf physiology routines" hydraulically-based [63]. These hydraulic representations considers vegetation species-specific structural characteristics and physiological traits, such as parameters related to internal plant functioning, including stomatal conductance. For a detailed description of the radiative processes, convection, and the water balance see [12].
VTUF-3D aims to assess the benefits of vegetation for climate sensitive urban design, considering vegetation abundance, type, and distribution [52].

The VTUF-3D model code runs on Ubuntu 14.04 with FORTRAN 2003 support, specifically gfortran 4.8.4. Furthermore, specific package versions are required for model configuration and post-processing, which may require manual installation as they are not intended for the use in Ubuntu 14.04 or outdated. Those packages include openjdk version "1.8.0_372", R version 3.6.3, and Python 3.4.3. The VTUF-3D source code can be obtained from [67].

3.3 VTUF-3D: Fix Parameters

In VTUF-3D, urban features are set to have the following characteristics due to limited user-friendliness. Thermal characteristics of structural materials are summarized in Table 3.4. An extended list of parameters can be found in Appendix B. This includes model integration, radiative, conduction, convection, domain geometry, building internal temperature, and loop parameters.

Table 3.4: Material thermal characteristics predefined in the VTUF-3D model (fixed parameters)

Parameter	Unit	Roof	Street	Wall
Albedo		0.15	0.1	0.3
Emissivity		0.92	0.92	0.88
Layer thickness	m	0.02, 0.02, 0.01, 0.03	0.02, 0.03, 0.1, 0.5	0.02, 0.03, 0.09, 0.02
Thermal Conductivity	W/mK	1.2, 1.2, 0.03, 1.5	0.8, 0.8, 0.9 ,0.3	1.1, 1.1, 1.1, 0.3
Volumetric Heat Capacity	MJ/m^3K	1.75, 1.75, 0.1, 2.25	2, 2, 1.5, 1.25	1.75, 2, 2, 1.5
Momentum roughness length	m	0.05	0.05	
Thermal roughness length	m	0.00025	0.00025	
Initial surface temperature	°C	18	23	22

Fixed soil parameters can be found in Table 3.5 and are further detailed in Appendix B. Soil thermal conductivity and heat capacity are calculated from soil porosity, water content, temperature, and organic matter [63].

Table 3.5: Soil characteristics predefined in the VTUF-3D model depending on vegetation species (fixed parameters)

Parameter	Unit	Turf grass	Brush box tree
Soil type		Loam	Loam
Albedo		0.2	0.2
Soil surface emissivity		0.95	0.95
Min thickness of dry soil layer	m	0.01	0.01
Tortuosity		0.66	0.66
Saturated soil hydraulic conductivity	mol/(m*s*MPa)	264.3	19.1
Soil porosity	m^3/m^3	0.38	0.43
Initial water content	m^3/m^3	0.06	0.3
Initial soil temperature	°C	15	15
Constant deep ground temperature	°C	20	20

A specification of the structural and species physiological parameters per predefined vegetation species applicable with VTUF-3D - Olive tree, Brush Box tree, and turf grass (Olea europaea, Lophostemon Confertus, and Festuca arundinacea) - can be found in the model publication, Table 4.3 and 4.4 [12].
In this thesis the Brush Box tree was used as tree representative for the Cool Square. Brush Box is an evergreen tree of up to 15 m height and 8 m width, commonly found in subtropical to tropical climates in Australia [68; 69]. Brush Box trees tolerate droughts lasting at max. six month with moderate supplementary watering [68; 69]. Preferred soil types are clay, loam, and sand [68]. The brush box tree is indicated for VTUF-3D with a leaf specific hydraulic conductance of 1.4e-4 kg.m-2.s-1.MPa-1.
The turf grass prefers a warm temperate climate, with a mean annual rainfall of 375 mm [70]. It tolerates wide soil characteristics [70]. The grass is indicated for VTUF-3D with a leaf specific hydraulic conductance of 1e-4 kg.m-2.s-1.MPa-1.

3.4 VTUF-3D: Input Parameters and Configuration for Heat/Cool Square Simulations

Urban micro-climate simulations are conducted for the Heat Square and the Cool Square design for meteorological forcing inputs measured on the 23/07/2022. An additional simulation for the Cool Square was conducted with meteorological forcing inputs measured on the 13/06/2023. The model configuration for those scenarios entails the following:

- the domain configuration based on the square designs,
- the meteorological forcing data,
- the height at which the forcing data is measured
- the study area co-ordinates

The meteorological forcing data must be measured above the max. building height and is here approximated to 6 m. The study area co-ordinates are (52N, 4.38E). The domain configuration and forcing data are further scenario specific model inputs and are described in the following subsections.

3.4.1 Domain Configuration

The study area description in VTUF-3D entails the following. A square study area is picked, in this case 46x46 m around the Heat/Cool Square. This is necessary as VTUF-3D assumes the surroundings of the study area to be replicas of the study area (homogeneous). The study area is described by a grid with grid patch attributes of building height, vegetation height, vegetation type, and tree number describing the study area form and features. Apart from size urban feature characteristics are set as fixed model parameters. Theoretically, feature characteristics of structural materials, soil, and vegetation can be adapted and expanded. However, the model code is chaotic and misses documentation which disabled this option for this works scope. Domain resolution, including height attributes of buildings and vegetation, are limited to integer values of unit meter. Hence, the grid size is chosen to the minimum of one meter.
The configuration for attributes is as follows: Building and vegetation heights are expressed as multiples of the grid size (attribute = object height / grid size). Grid patches with building height and vegetation types attributed to zero are considered to be a road features. Vegetation attributes cannot be allocated for patches with buildings and vice versa.
Patches with vegetation get assigned a vegetation height, type, individual tree number and with that tree number also the crown extent. The predefined vegetation types include grass (attribute number = 2), olive tree (attribute number = 1), and brush box (attribute number = 3). The specification of a tree type for a grid patch is treated as the tree stem. With the attribute 'tree number' the extent of the tree crown can be described. Each tree gets assigned a unique tree number for identification of the individual trees. The configuration format to be read in by VTUF-3D can be found in Appendix C.

A visualization of the Heat Square design configured as model domain is shown in Figure 3.4. Similarly, the Cool Square configuration is shown in Figure 3.5. The statistics for the domain area characteristics of Heat and Cool Square are summarized in Table 3.6.

Table 3.6: Statistics for the domain characteristics of Heat and Cool Square based on the model domain configuration

Characteristic	Unit	**Heat Square**	**Cool Square**
Trees	%	0	0.4
Grass	%	23	38
Building	%	20	20
Streets	%	57	42
Mean vegetation height	m	0.00	4.10
Mean building height	m	4.32	4.33

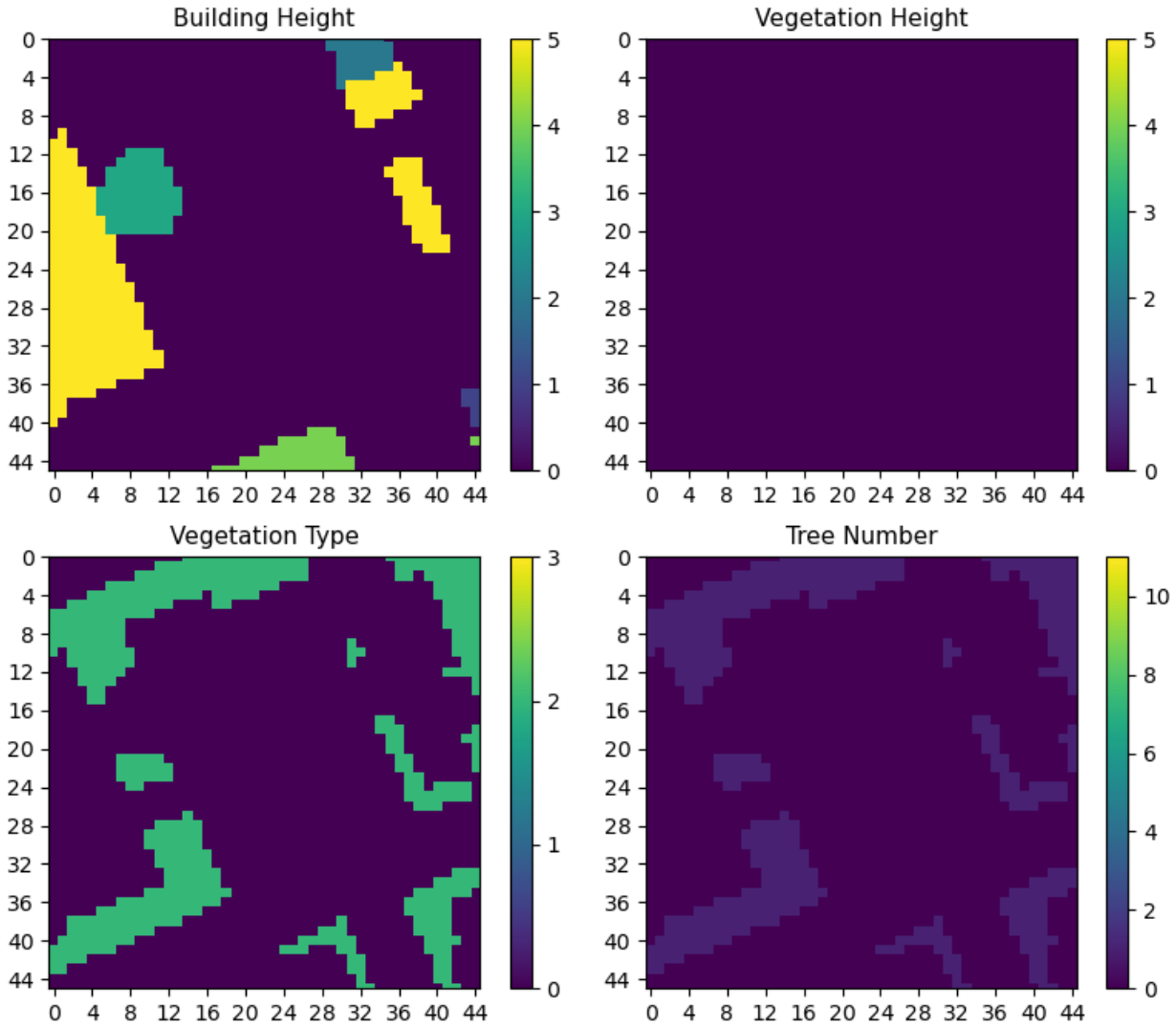

Figure 3.4: Heat Square configuration per attribute. Study area is 45x45 m, with grid size of 1 m. Height attribute unit is meter. All attribute values are integers.

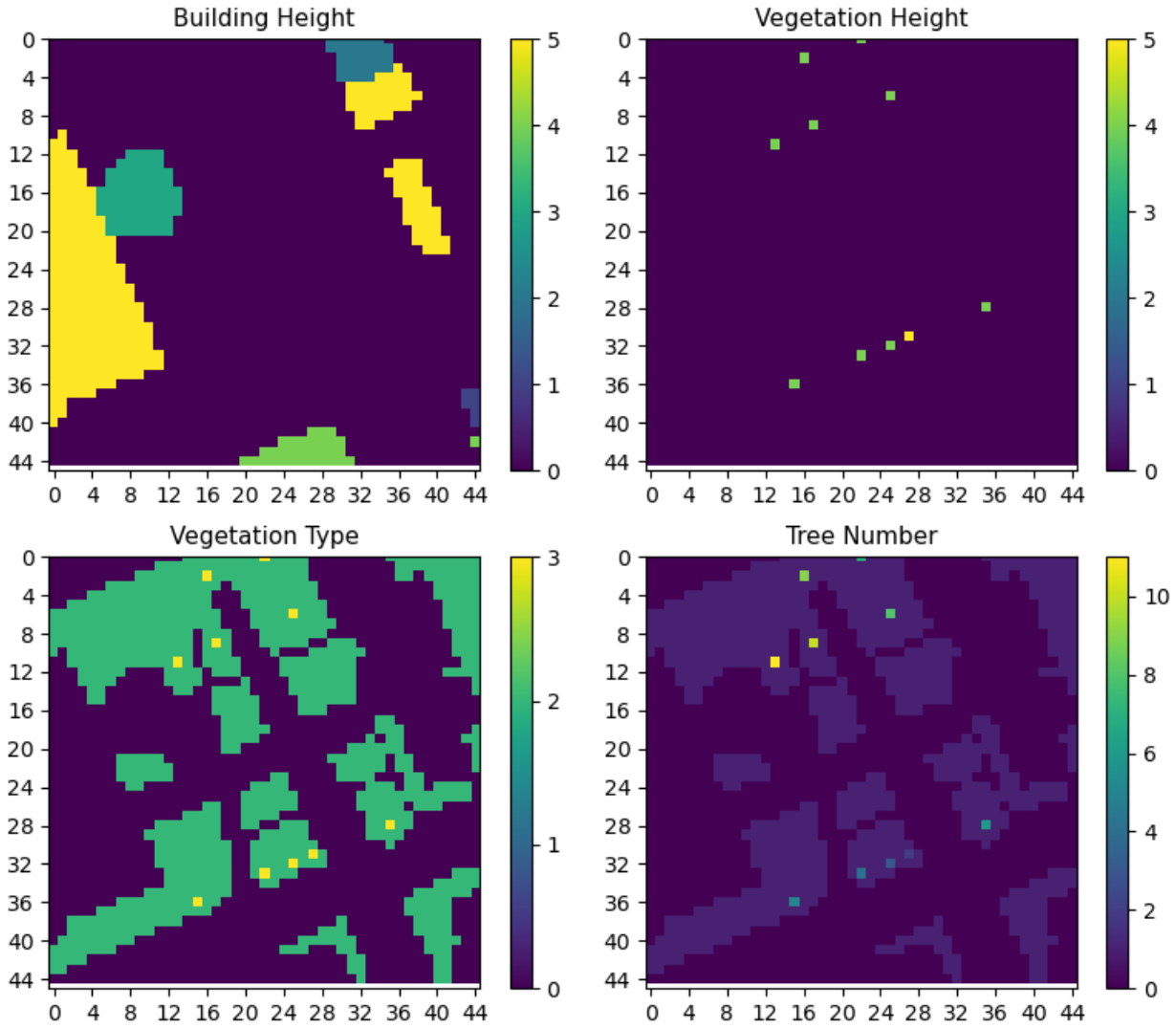

Figure 3.5: Cool Square configuration per attribute. Study area is 45x45 m, with grid size of 1 m. Height attribute unit is meter. All attribute values are integers.

3.4.2 Forcing Data and Configuration

VTUF-3D takes meteorological measurements as simulation forcing data. The 23/07/2022 and the 13/06/2023 are both clear summer days. For those days 24 hours of half-hourly forcing data was prepared from the measured weather conditions. This meteorological forcing input includes:

- Downwelling shortwave radiation [W/m²]
- Downwelling longwave radiation [W/m²]
- Wind speed, east [m/s]
- Wind speed, north [m/s]
- Air pressure [Pa]
- Air temperature [K]
- Absolute humidity [kg/kg]
- Rainfall [kg/m²/s]
- Snowfall [kg/m²/s]

The forcing data is specified with the measurements taken on and around the square. Rainfall is specified by measurements taken with the Davis Weather Station, downwelling longwave radiation is specified by measurements taken with the CR6 radiometer, the rest of the forcing data is specified by measurements of the weather station of the co-creation center. See Table 3.3 and Figure 3.2a for Device locations.
Unit conversion is required for parameters air pressure, air temperature, and rainfall. Additionally, the specific humidity must be calculated from relative humidity, air temperature, and air pressure. Therefore, the saturation vapour pressure is calculated using the Magnus-Tetens Equation 3.1. With equation 3.2 the vapour pressure is calculated. The specific humidity is derived from Equation 3.3. The east and north wind is calculated with the wind speed vector decomposition using Equations 3.4 and 3.5. The forcing data must be presented with a negative UTC offset of 10 hours. The forcing data and layout can be found in Appendix C. The meteorological forcing data for 23/07/2022 is visualized in Figure C.1. The visualization of the meteorological forcing data for 13/06/2023 can be found in Appendix C.

$$es = 6.112 * \exp\left(\frac{17.67 * T_a}{T_a + 243.5}\right) \tag{3.1}$$

$$e = es * \frac{RH}{100} \tag{3.2}$$

$$q = 0.622 * \frac{e}{P_a - e} \tag{3.3}$$

$$V_E = \sin\theta * -V \tag{3.4}$$

$$V_N = \cos\theta * -V \tag{3.5}$$

with
es - Saturation vapour pressure [kPa]
e - Vapour pressure [kPa]
T_a - Air temperature [°C]
RH - Relative humidity [%]
q - Specific humidity [kg/kg]
P_a - Air pressure [kPa]
V_E - East wind [m/s]
V_N - North wind [m/s]
θ - Wind direction [°]
V - Wind speed [m/s]

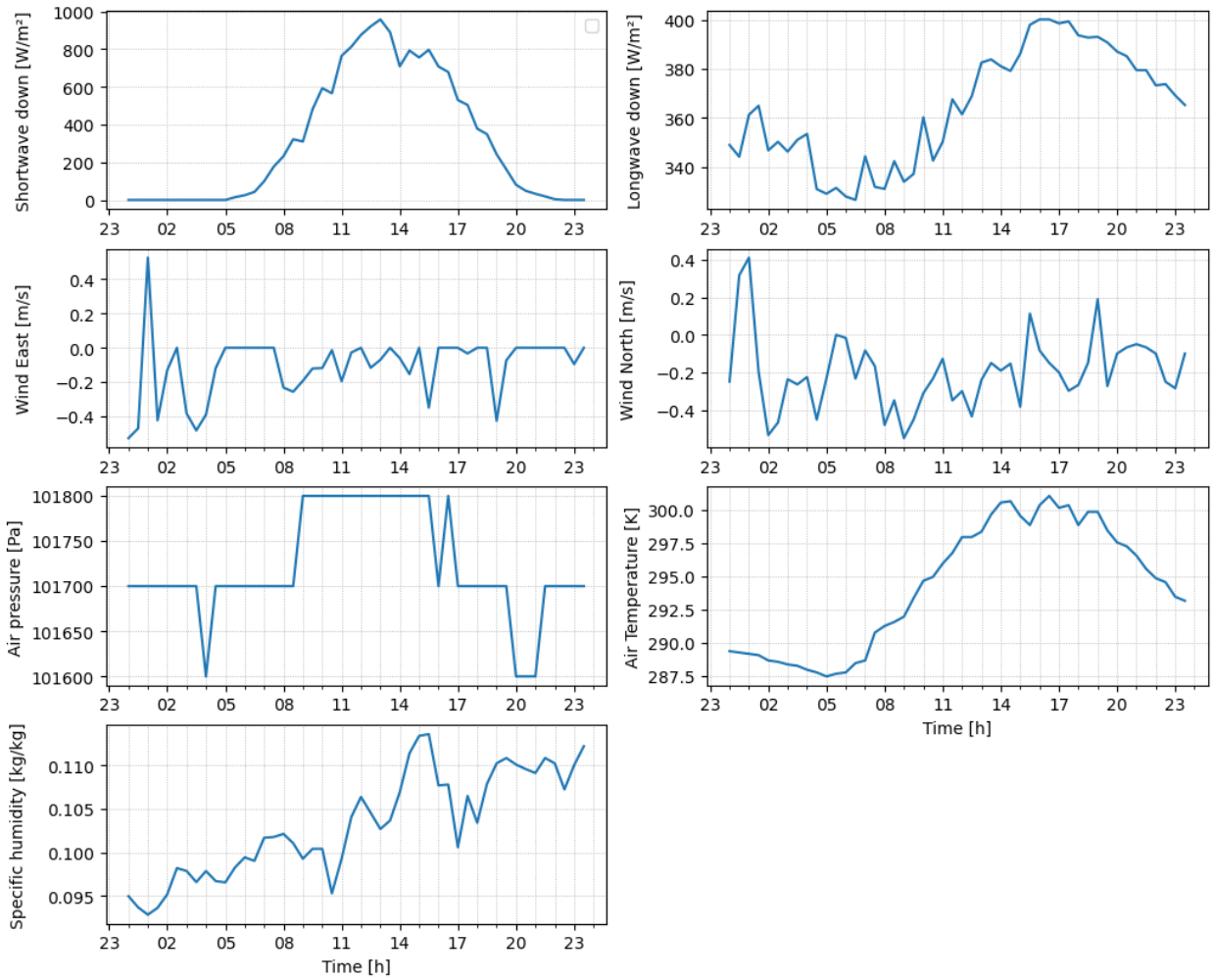

Figure 3.6: Meteorological forcing data 23/07/2022

3.5 Model Output and Assessment

VTUF-3D calculates hourly time series data for a number of output parameters. Following, the model output used in this thesis as well as meteorological measurements used for validation are specified. Please find a summary of additional model output parameters in Appendix D. Furthermore, this section provides the approach for the simulation validation and assessment of heat mitigation from the Heat to the Cool Square design.

3.5.1 Model Output Validation

This section describes the approach used for validating the model outputs from the Heat and Cool Square simulations. The model output is compared to meteorological measurements taken at the square in terms of coefficient of variation (COV) and diurnal pattern (visual assessment). Further evaluation of the model output entails the impact evaluation of differentiating model feature characteristics from the square characteristics, and limitations in model calculations.

Heat Square Simulation Validation

The Heat Square was simulated for weather conditions on the 23/07/2022. For validation, the model output is compared to the meteorological measurements taken on the square on the same date. Table 3.7 shows the parameter specification for the observations vs. model output. Observations are specified with measurement devices in brackets. See 3.3 for specific device locations on the square.

Table 3.7: Heat Square model output and measurements specification for comparison, related to paved surfaces.

Observations	Model output
Upwelling longwave radiation measured above concrete ($LW_{up-con,o}$) (CR6 radiometer)	Upwelling longwave radiation modelled, square average ($LW_{up,m}$)
Upwelling shortwave radiation measured above concrete ($SW_{up-con,o}$) (CR6 radiometer)	Upwelling shortwave radiation modelled, square average ($SW_{up,m}$)
Concrete surface temperature measured ($T_{con,o}$) (Testo 176T4)	Road surface temperature modelled, square average ($T_{road,m}$)
Canyon air temperature measured 1.4 m above concrete ($T_{air-con,o}$) (Testo 174H)	Canyon air temperature modelled, square average ($T_{air,m}$)

Cool Square Simulation Validation

For the Cool Square design measurements for validation exists for the 13/06/2023 and 15/06/2023, both dates showing similar weather conditions. Hence, the Cool Square model output for weather conditions of the 13/06/2023 is compared with the measurements from both dates. Find the specification of the observations and model output for comparison in Table 3.8.

Table 3.8: Cool Square model output and measurements specification for comparison, related to paved surfaces.

Observations	Model output
Traditional pavement surface temperature measured ($T_{pav,o}$) (176T4)	Road surface temperature modelled, square average ($T_{road,m}$)
Canyon air temperature measured above traditional pavement ($T_{air-pav,o}$)	$T_{air,m}$
Upwelling shortwave radiation measured above traditional pavement ($SW_{up-pav,o}$) (NR01 radiometer)	$SW_{up,m}$
Upwelling longwave radiation measured above traditional pavement ($LW_{up-pav,o}$) (NR01 radiometer)	$LW_{up,m}$

Table 3.9: Cool Square model output and measurements specification for comparison, related to grass patches.

Observations	Model output
Soil surface temperature measured on grass patch ($T_{sfc-soil,o}$) (176T4)	Soil temperature of top layer (0.1 m) for grass patch modelled ($T_{soil,m}$)
Canyon air temperature measured above grass ($T_{air-grass,o}$)	Canyon air temperature above grass modelled ($T_{air-grass,m}$)
Soil moisture measured at -8 cm for grass patch ($\theta_{soil,o}$) (Teros 12)	Soil moisture modelled for grass patch ($\theta_{soil,m}$)
Upwelling shortwave radiation measured above grass ($SW_{up-grass,o}$) (NR01 radiometer)	Upwelling shortwave radiation modelled, square average ($SW_{up-grass,m}$)
Upwelling longwave radiation measured above grass ($LW_{up-grass,o}$) (NR01 radiometer)	Upwelling longwave radiation modelled, square average ($LW_{up-grass,m}$)

3.5.2 Evaporative Cooling Assessment

To evaluate the climate effects from Heat to Cool Square, the model output for the Heat and Cool Square simulations are compared. All model output refers to the simulation with the meteorological forcing from the 23/07/2022.

The evaluation includes radiation and temperature changes; the difference in the spatial distribution of surface temperatures; the comparison of sensible, ground, and latent heat fluxes; as well as wind speed deviations; and the effect on the HTC via UTCI. Thereby, the result accuracy established in the simulation validation and model limitations are taken into account.

4 Green Village Case Study: Results and Discussion

This chapter presents the Heat and Cool Square simulation results of VTUF-3D and their comparison with observations for validation (section 4.1 and 4.2). Additionally, Heat and Cool Square simulation results are compared for cooling effect assessment in section 4.3. Finally, section 4.4 presents further considerations for model application. Note that all material properties referred to are described in section 3.1.1 and 3.3.

4.1 Heat Square Simulation Validation

The Heat Square simulation was conducted for weather conditions on the 23/07/2022, with the respective meteorological input described in section 3.4.2. Here, the calculated model output is compared with the respective meteorological measurements of the Heat Square taken on 23/07/2022. Figure 4.1 shows the simulated and observed time series data for upwelling shortwave and longwave radiation, surface and air temperature as introduced in 3.5.1.

Apart from air temperature, the model output does not align with the measurements. The modelled upwelling shortwave radiation $SW_{up,m}$ shows a COV of 1.19 compared to $SW_{up-con,o}$. The ground surface temperature shows a COV of 0.29 for $T_{road,m}$ compared to $T_{con,o}$. During the day $T_{road,m}$ is up to 10 °C higher than $T_{con,o}$, starts to increase and peaks quicker. The values during the night fit the observations. $T_{soil,m}$ shows unexpected values after 7 PM, going below 0 °C. The upwelling longwave radiation comparison of $LW_{up,m}$ to $LW_{up-con,o}$ shows a COV of 0.08. $LW_{up,m}$ is at most 70 W/m² higher than $LW_{up-con,o}$, increases and peaks quicker. During the night the values are similar. The canyon air temperature shows a COV of 0.06 for $T_{air,m}$ compared to $T_{air-con,o}$. Simulations and observations follow the same course.

The deviation of $SW_{up,m}$ from $SW_{up-con,o}$ is likely due to the low model road albedo of 0.1 compared to the measured concrete albedo of 0.31.
The deviation of $T_{road,m}$ from $T_{con,o}$ appears to be a result of the low model road albedo as well. Additional influences could be the lower model road heat capacity (2 MJ/m³K) than literature suggests for the concrete (2 - 2.8 MJ/m³K) on the Heat Square. Although, the thermal conductivity of the model road is higher than literature suggests for concrete.
The deviation of $LW_{up,m}$ from $LW_{up-con,o}$ relates to the overestimation of $T_{road,m}$ compared to $T_{con,o}$, as emissivity values for simulation and observation are similar. $T_{soil,m}$ does not appear to drive $LW_{up,m}$ as $T_{soil,m}$ does not translate into the the pattern of $LW_{up,m}$. That might be due to vegetated area uptake of only 23%, although $T_{soil,m}$ is considerably lower than $T_{road,m}$ and shows a lower emissivity as well. However, the calculation of $T_{soil,m}$ is also questionable since it produces unexpected negative results.
$T_{road,m}$ would suggest that $T_{air,m}$ is an overestimation. However, this does not show, likely because $T_{air,m}$ is an average value for the air temperature below the mean building height (4.32 m) [12]. $T_{air-con,o}$ was measured at the 1.4 m above the ground. $T_{air,m}$ is driven by the difference in temperature of surface and air in combination with the convective heat transfer coefficient and the heat capacity of air [12]. Air pressure, temperature, and humidity influencing those components are considered in the model, hence the main cause is likely the temperature averaging.

In summary, the low model road albedo can be identified as a strong driver of the model output inaccuracy for the Heat Square. Additionally, $T_{air,m}$ seems to be too broad a parameter.

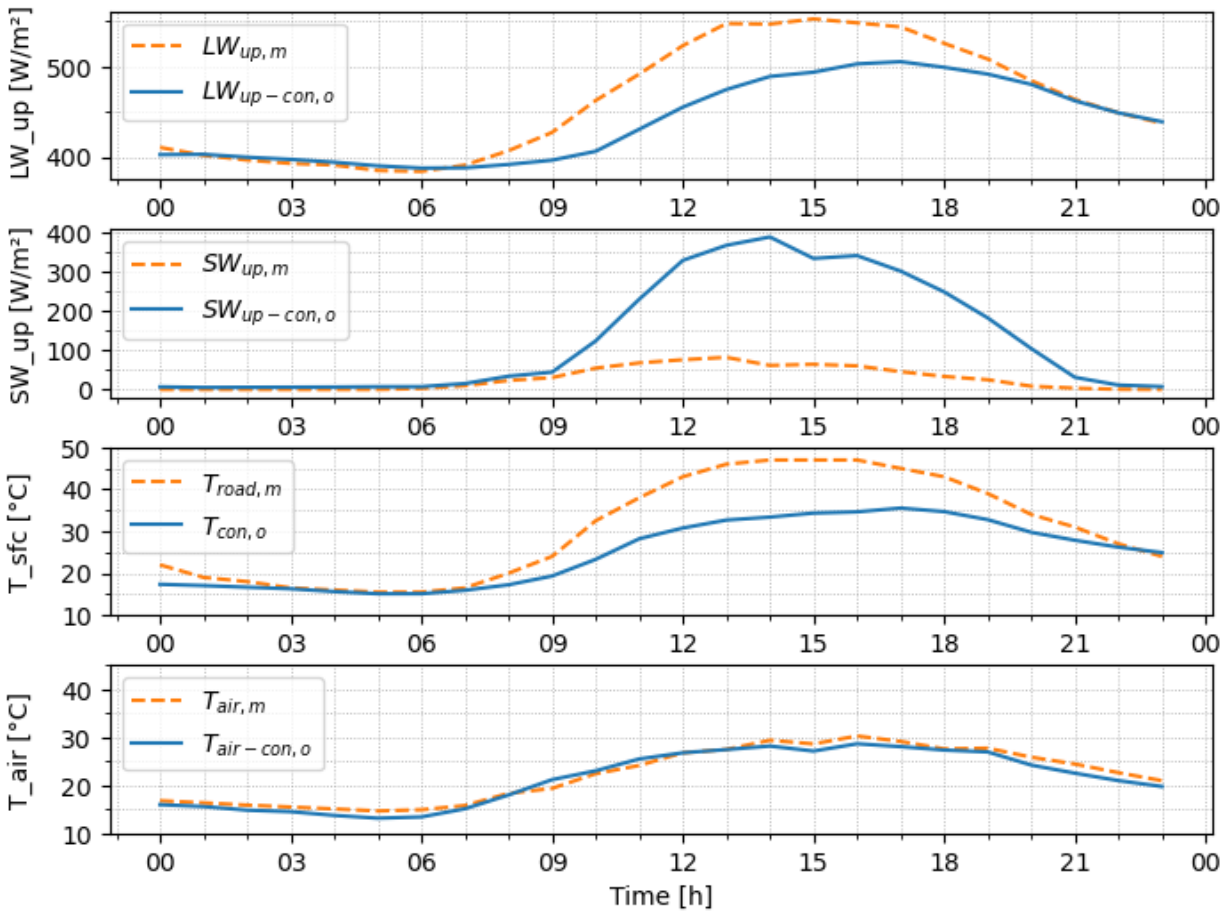

Figure 4.1: Heat Square model output vs. observations, from top to bottom: Upwelling longwave radiation $LW_{up,m}$ and $LW_{up-con,o}$; Upwelling shortwave radiation $SW_{up,m}$ and $SW_{up-con,o}$; Road temperature $T_{road,m}$ and $T_{con,o}$; Canyon air temperature $T_{air,m}$ and $T_{air-con,o}$

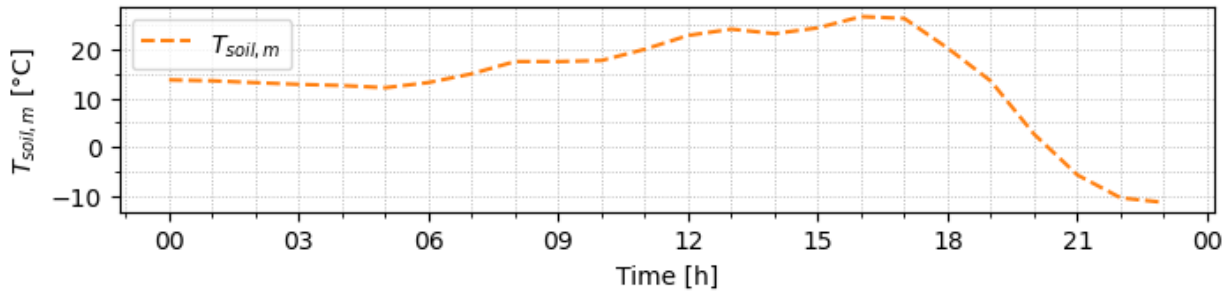

Figure 4.2: Heat Square model output for $T_{soil,m}$

4.2 Cool Square Simulation Validation

This section compares the Cool Square simulation results with measurements on the square for simulation validation. Therefore, a Cool Square simulation was conducted on the 13/06/2023. Meteorological measurements at the Cool Square exist for the 13/06/2023 and the 15/06/2023. Both dates show similar weather conditions. These observations are used for comparison with the calculated model output as

introduced in 3.5.1. For comparison, the observation and simulation results are displayed in Figure 4.3. They show the observed vs. simulated time series values of upwelling longwave and shortwave radiation, air and surface temperature, and soil moisture related to grass patches and paved surfaces.

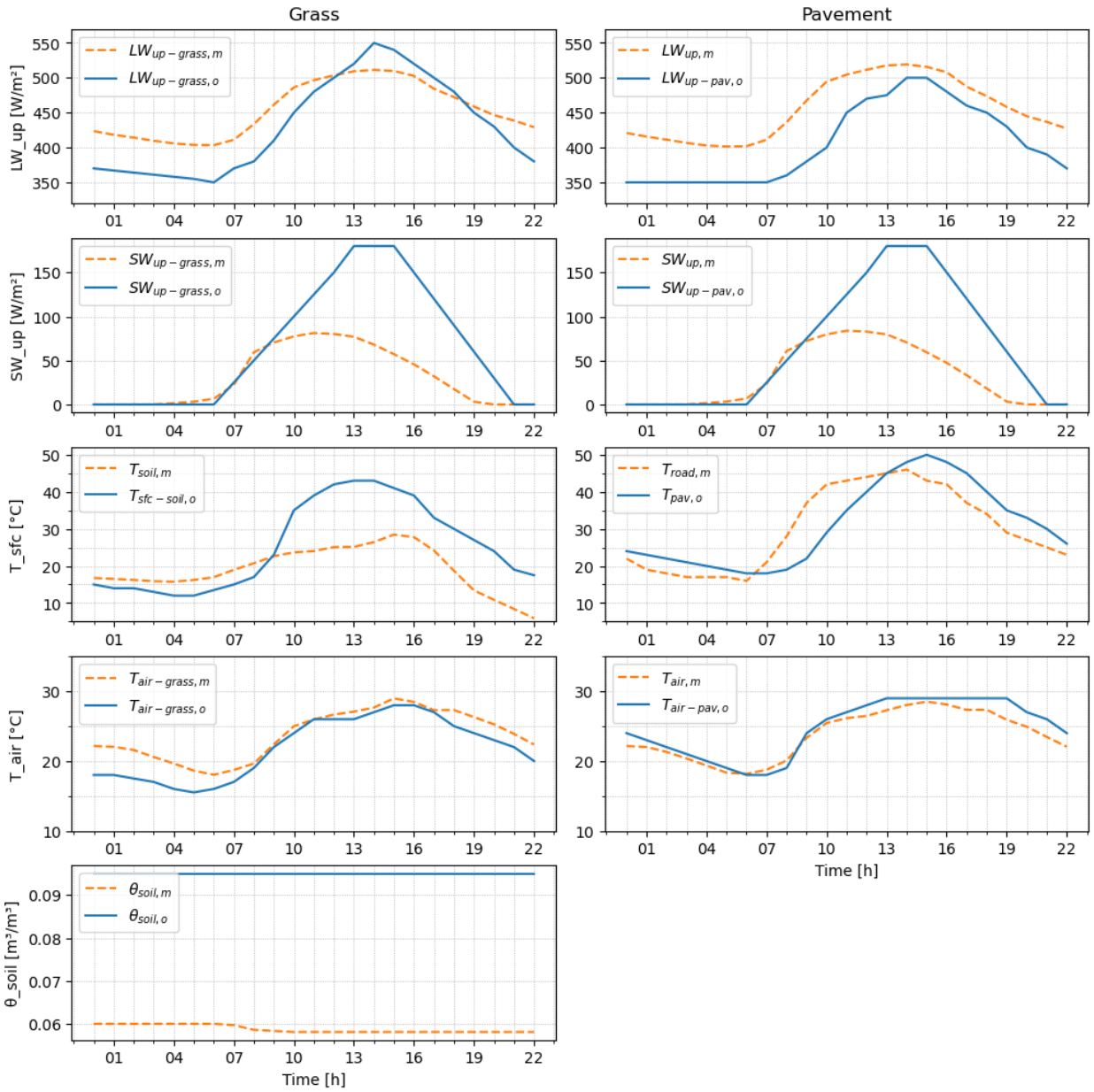

Figure 4.3: Cool Square model output vs. observations for grass (left) and pavement (right). From top to bottom: upwelling longwave and shortwave radiation, surface and air temperature, soil moisture (Grass only). Parameter specification in Table 3.8 and 3.9.

First, the results related to grass. The model output does not align with the measurements taken on the Cool Square. $LW_{up-grass,m}$ has a COV of 0.09 compared to $LW_{up-grass,o}$, with an overestimation of 50 W/m² during the night and morning and an underestimation of the peak by 50 W/m². $SW_{up-grass,m}$ shows a COV of 0.86 compared to $SW_{up-grass,o}$, underestimating the peak and peaking earlier. $T_{soil,m}$ has a COV of 0.41 compared to $T_{sfc-soil,o}$, peaking 15 °C lower and underestimating the hours after 9 AM. $T_{air-grass,m}$ has a COV of 0.11 compared to $T_{air-grass,o}$, overestimating the night temperatures by 5 °C. $\theta_{soil,m}$ shows a COV of 0.9 compared to $\theta_{soil,o}$, underestimating the soil moisture by 0.94 m³/m³.

Second, the results related to paved surface. The model output for radiation deviates from the measurements, whereas temperature values fit in magnitude. $LW_{up,m}$ shows a COV of 0.13 compared to $LW_{up-pav,o}$, overestimating the upwelling longwave radiation by up to 100 W/m². $SW_{up,m}$ shows a COV of 0.84 compared to $SW_{up-pav,o}$, equal to $SW_{up-grass,m}$. $T_{road,m}$ has a COV of 0.21 compared to $T_{pav,o}$. It shows a diurnal pattern shift of 2 hours earlier and peaks 5 °C lower than $T_{pav,o}$. $T_{air,m}$ shows a COV of 0.06 compared to $T_{air-pav,o}$, underestimating the day time values.

In the following, the deviations of the simulations from observations for grass areas are discussed. $SW_{up-grass,m}$ is half of $SW_{up-grass,o}$ although both, model and measured albedo are specified with 0.2. Since $SW_{up-grass,m}$ is equal to $SW_{up,m}$ it is likely that VTUF-3D uses the road albedo of 0.1 for grass areas as well.
When comparing $T_{soil,m}$ with $T_{sfc-soil,o}$, it is important to note that $T_{sfc-soil,o}$ represents the measured soil surface temperature, whereas $T_{soil,m}$ corresponds to the modelled soil temperature in the first layer (0.1 m). The model soil absorbs more heat because the model soil emissivity and hence absorption is specified with 0.95 compared to the 0.85 measured. The heat capacity and conduction depends on the soil moisture content. Since $\theta_{soil,m}$ is 0.04 m³/m³ lower than $\theta_{soil,o}$ the heat capacity and conduction is likely lower than in reality, in case of a similar soil type. Additionally, with $\theta_{soil,m}$ being lower than $\theta_{soil,o}$ the modelled surface cooling soil evaporation is expected to be lower than in reality. Hence, the soil temperature should not differ as much, considering the layer temperature averaging of $T_{soil,m}$. However, the temperature averaging is a potential explanation for $T_{soil,m}$ being higher in the night and lower in the day. The strong decrease in the evening is still interesting though as $T_{air-grass,m}$ does not drop under 22 °C and the constant deep soil temperature is 20 °C. These evening values are not plausible.
$LW_{up-grass,m}$ is an overestimation of the reality during the night and morning. This is likely because $LW_{up-grass,m}$ is a result of soil temperature and emissivity and the model soil emissivity is higher than the measured emissivity. $T_{soil,m}$ does not peak as high as $T_{sfc-soil,o}$. Hence, the peak underestimation by $LW_{up-grass,m}$. In the evening, $LW_{up-grass,m}$ does not relate to the $T_{soil,m}$ anymore. $T_{soil,m}$ drops to 5 °C while $LW_{up-grass,m}$ stays up. This is not plausible and suggests that $LW_{up-grass,m}$ is based on $T_{road,m}$ rather than $T_{soil,m}$ as it relates to $LW_{up,m}$, which follows the pattern of $T_{road,m}$.
$T_{air-grass,m}$ follows the pattern of $T_{air-grass,o}$ during the day. However, based on the similarity of $T_{air-grass,m}$ with $T_{air,m}$, it can be assumed that the two parameters are the same. Since $T_{air-grass,m}$ does not relate to the pattern of $T_{soil,m}$, it can be assumed that $T_{air-grass,m}$ is $T_{air,m}$ and relates to $T_{road,m}$.
Finally, the model underestimates $\theta_{soil,o}$. This is likely due to the model parameter for initial soil water content of 0.06 m³m³. Note that $\theta_{soil,o}$ likely shows a drop in values during the day as well. This is underlined by reported measurements where soil moisture drops are visible, but the scale forbids the identification of the specific timing [56].

In the following, the deviations of the simulations from observations for paved surfaces are discussed. $SW_{up,m}$ is an underestimation of $SW_{up-pav,o}$ because of the model road albedo of 0.1 compared to the measured albedo for the traditional pavement on the Cool Square of 0.23. The time pattern difference could be due to a significant albedo change of the ground surface with the angle of the downwelling shortwave radiation. The premature pattern of $SW_{up,m}$ translates to $T_{road,m}$ and $LW_{up,m}$. There is no deviation in thermal capacity and conductivity from the model to observations. Hence, these parameters are not effecting the diurnal pattern.
$T_{road,m}$ likely fits $T_{pav,o}$ in magnitude because of the lower model albedo in combination with the higher model absorption compared to the measured albedo and emissivity.
$LW_{up,m}$ is overestimating $LW_{up-pav,o}$ likely because of the higher model road and soil emissivity (0.92 and 0.95) compared to the measured emissivity of the traditional pavement on the Cool Square (0.83). $T_{road,m}$ drives $LW_{up,m}$ only with the earlier time pattern compared to $T_{pav,o}$, because $T_{road,m}$ shows the same magnitude as $T_{pav,o}$.
That $T_{air,m}$ fits $T_{air-pav,o}$ is curious because $T_{road,m}$ and $T_{pav,o}$ show the same magnitude ($T_{soil,m}$ is even lower). Therefore, $T_{air,m}$ is expected to be lower than $T_{air-pav,o}$ because $T_{air,m}$ represents an averaged value below height 4.32 meter. $T_{air,m}$ depends on the sensible heat flux and the heat capacity of air [12]. The calculation of the heat capacity with VTUF-3D is not specified in the publication. Deviations from the reality for the heat capacity parameter could have influenced $T_{air,m}$.

In summary, the validation of the model output for the Cool Square simulation suggests that model parameters for albedo, emissivity, and initial soil moisture are strong drivers of mismatches between model output and measurements. Additionally, striking is that $T_{soil,m}$ does not seem to relate to downwelling and upwelling radiation nor air temperature. Moreover, modelled upwelling radiation and air temperature over vegetated areas appear to be based on material parameters of the model road. This suggests confusion related to model output parameter ambiguity.

4.3 Comparison of Heat and Cool Square

This section presents a comparison of the Heat and Cool Square simulation results using VTUF-3D. Both simulations were carried out with meteorological measurements from the 23/07/2022 as forcing data. The model output for Heat and Cool Square are compared for cooling assessment, considering the model output accuracy discussed in sections 4.1 and 4.2.

4.3.1 Radiation and Temperatures

Figure 4.4 shows the model output for the square averages of the upwelling shortwave and longwave radiation, ground and air temperature for the Heat and Cool Square. The simulation results show an increased $SW_{up,m}$ from Heat to Cool Square. $LW_{up,m}$ and Ground surface temperature modelled, square average ($T_{ground,m}$) drop from Heat to Cool Square. $T_{air,m}$ remains the same.

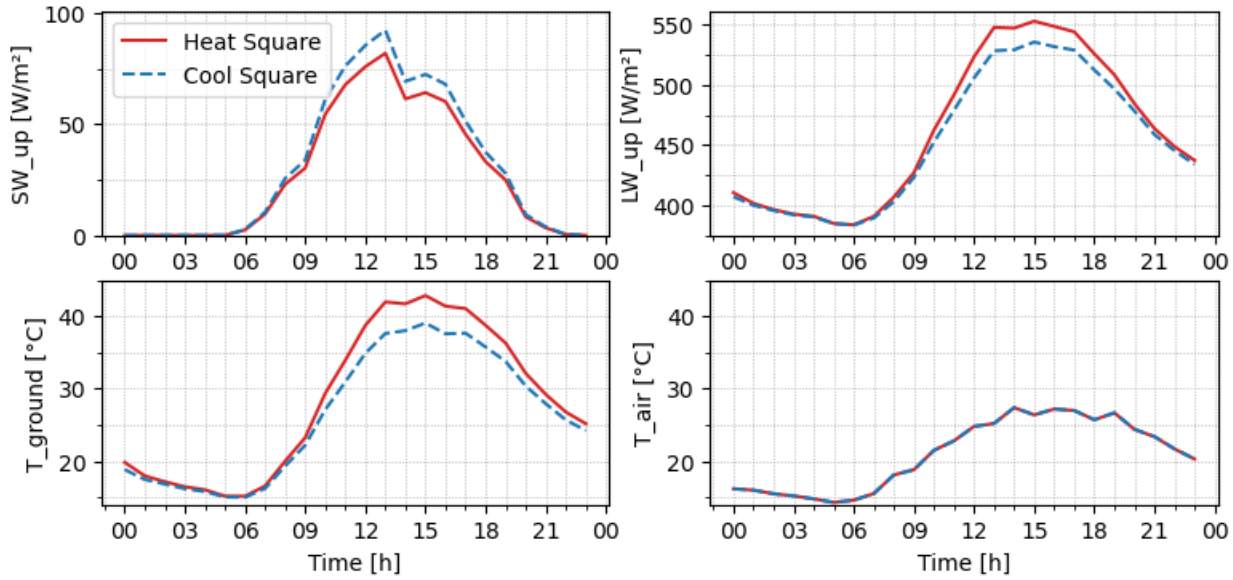

Figure 4.4: Model output of Heat and Cool Square for upwelling shortwave (top left) and longwave radiation (top right), ground temperature (bottom left) and air temperature (bottom right). Values are square averages.

The increased $SW_{up,m}$ from Heat to Cool Square is a result of an increased vegetated area with a model albedo of 0.2 compared to the model road albedo of 0.1. So, this is plausible for the model output given the model parameters. However, $SW_{up,m}$ for Heat and Cool Square should be larger, based on the square characteristics measured and suggested from literature. Also, $SW_{up,m}$ for the Heat Square should over-top $SW_{up,m}$ from the Cool Square.
Knowing that $T_{road,m}$ for the Heat Square is an overestimation $T_{ground,m}$ likely is too. And given the above consideration, $T_{ground,m}$ of the Cool Square should be higher. $T_{ground,m}$ of the Cool Square should be

between 45 °C and 50 °C, as indicated by the measurements at the Cool Square on the 13/06/23 and 15/06/23. So, the average ground surface temperature of the Cool Square should be higher than the Heat Square. That the model configuration does not show the expected trend is plausible.
The square characteristics measured suggest a drop in emissivity from Heat to Cool Square. However, with the expected ground temperatures, discussed above, the upwelling longwave radiation for the Cool Square should be higher than for the Heat Square.
$T_{air,m}$ remains equal from Heat to Cool Square. This is likely due to the air temperature averaging over the canyon height. Otherwise, $T_{ground,m}$ would suggest a significant difference in air temperature. Given the observations, the air temperature should be higher for the Cool Square compared to the Heat Square. That is assuming the influence of humidity to be neglectable.

Figure 4.5 illustrates the surface temperature distribution of the Heat Square (4.5a) and the Cool Square (4.5b) at 4 PM. 4 PM is the time of the highest simulated surface temperature values. The surface temperature distribution shows similar values for the Heat and Cool Square, except for the areas with added vegetation. Areas of vegetation, no matter the type, show a temperature of approximately 27 °C. Building features show the highest temperatures of up to 55 °C. The road temperature is about 48 °C.

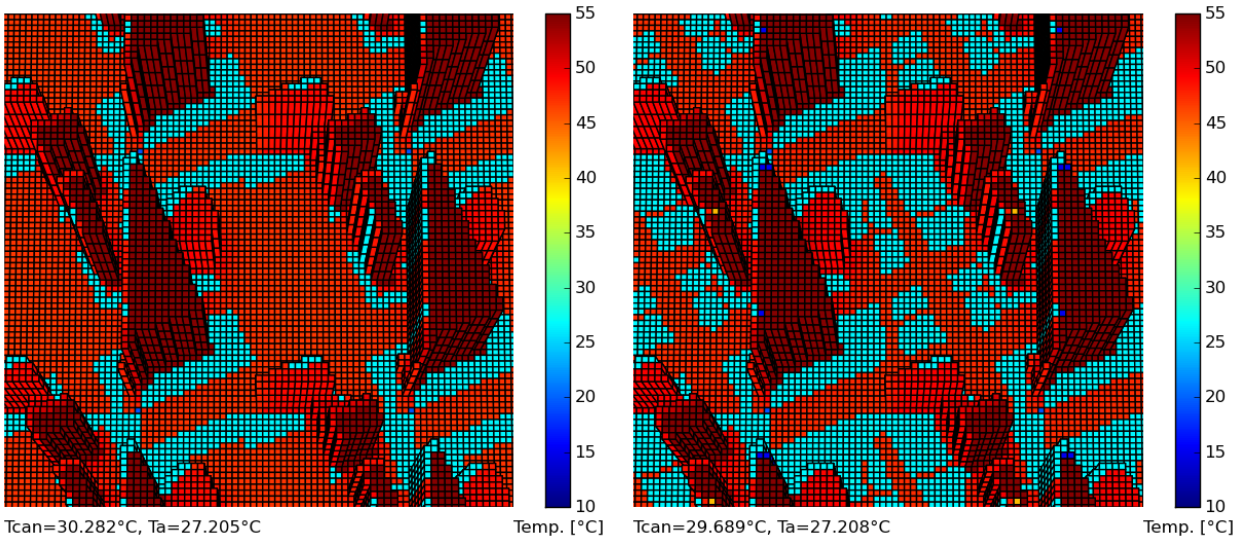

(a) Heat Square

(b) Cool Square

Figure 4.5: Surface temperature distribution for Heat (4.5a) and Cool Square (4.5b) at 4 PM. For reference, average canopy and air temperature values are indicated. Grid size is 1 m.

Figure 4.5 suggests that the spatial distribution of the model output goes as far as feature type and feature orientation. The model output parameters indicated in Appendix D support this assumption. Model output is averaged per defined domain characteristic and orientation, including shading and position towards other domain features. Feature temperatures for bright surfaces exist as output parameters as well, these are not included in the spatial distribution though. This may be a drawback in the spatial assessment of heat mitigation.
However, Figure 4.5 is useful for the assessment of temperature differences between surfaces and the air. A temperature gradient assessment is not possible since the modelled air temperature is averaged below the mean building height. The output suggests the strongest temperature difference for building features during the day. However, the accuracy of this result can not be evaluated, since observations for the building characteristics are unknown. The lowest temperature difference is suggested for the vegetated areas. Interestingly, no differences between vegetation species can be observed in Figure 4.5. This is likely because vegetation temperatures are averaged over the area. With VTUF-3D aiming to assess the impact of greening for climate sensitive urban design, a more apparent way to see the species benefits would be expected. Note, the individual vegetation species effects are presented in a separate model output file, see Appendix D.

Figure 4.5 suggests a drop in average ground surface temperature from Heat to Cool Square. Given the model output accuracy, the paved surface temperatures - especially for the Heat Square - are likely lower and the vegetated surface temperatures likely higher. Hence, the temperature differences changes from Heat to Cool Square are expected to be smaller and therewith less of a heat mitigation driver.

In summary, the deviation of model parameters for the square characteristics lead to unexpected values for upwelling radiation and surface temperatures. In relation to the Heat Square, Cool Square values for upwelling shortwave radiation are overestimated and ground surface temperature and upwelling longwave radiation are underestimated. The assumption for the air mixing rate is once more identified as problematic for air temperature assessment at human level. Furthermore, the spatial surface temperature assessment with VTUF-3D is limited in spatial relations of urban characteristics and by averaging vegetation species effects. However, it is a useful indicator for temperature gradients assessment per domain characteristic, given result accuracy. For the Cool Square, ground surface temperatures are expected to be less of a driver for heat mitigation compared to the Heat Square.
It is recommended to improve the model configuration regarding the material and vegetation properties for the assessment of the greening impact on the heat mitigation from Heat to Cool Square. Second, it is recommended to improve the spatial temperature assessment with VTUF-3D for a more apparent impact visualization of vegetation species.

4.3.2 Heat Fluxes

Figure 4.6 illustrates the simulated heat fluxes for the Heat and Cool Square. These include sensible, ground, and latent heat flux averaged over the square.

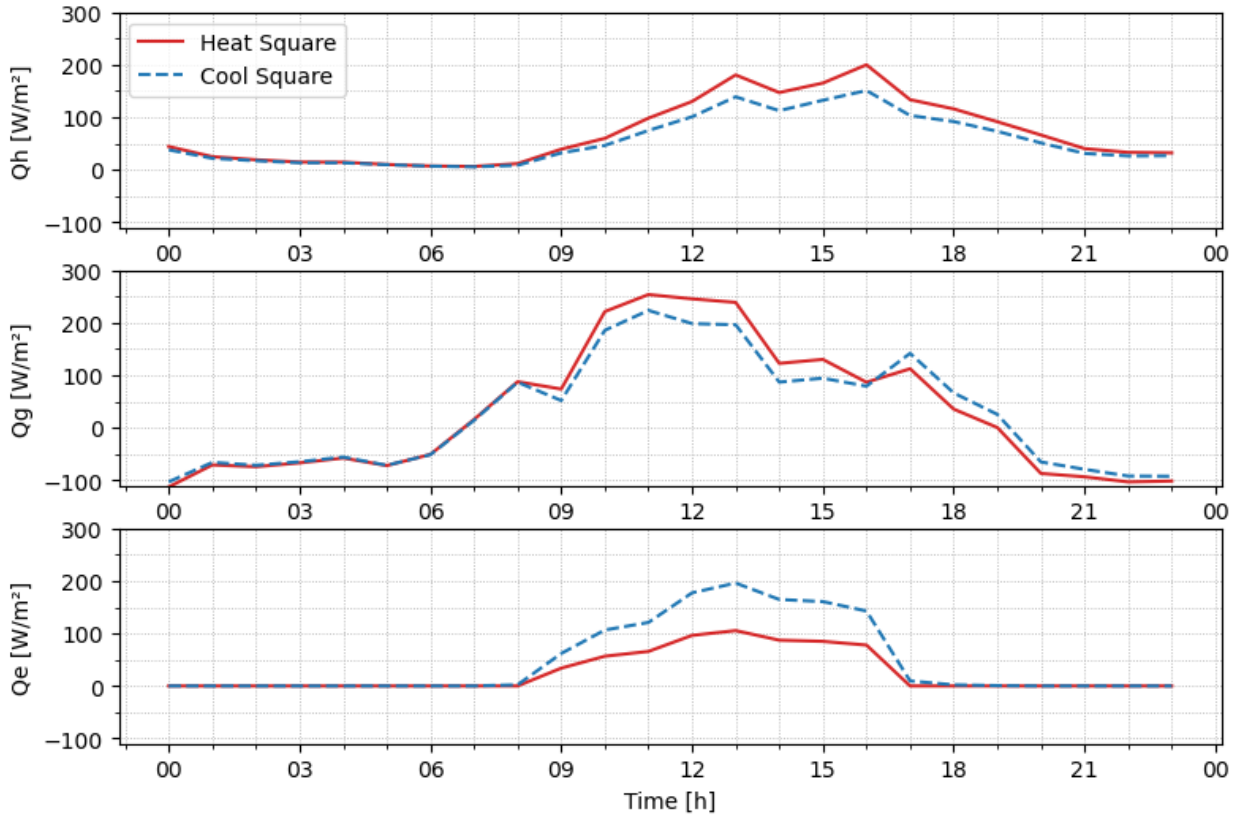

Figure 4.6: Model output for Heat and Cool Square, from top to bottom: sensible heat flux (Qh), ground heat flux (Qg), and latent heat flux (Qe). Results are square averages.

The sensible heat flux is reduced for the Cool Square from 9 Am to 9 PM, with a maximum offset of 50 W/m² from 1 to 4 PM. The night shows similar magnitudes. The ground heat flux for the Cool Square simulation shows reduces values from 9 AM to 6 PM, with a maximum offset of 50 W/m². From 7 to 12 PM the Cool Square ground heat flux is higher by a magnitude of maximum 30 W/m². The simulated latent heat flux is 0 before 8 AM and after 6 PM for both square configurations. For the Heat Square the latent heat flux increases up to 110 W/m² at 1 PM. The Cool Square shows an increase of latent heat up to 200 W/m² at 1 PM.

The model output suggests that the sensible and ground heat flux decrease from Heat to Cool Square, based on the modelled ground surface temperature decrease. However, as discussed above the ground temperature is expected to be higher for the Cool Square, considering all paved surfaces on the Cool Square as traditional pavement. The Cool square shows a higher variability in characteristics as introduced in section 3.1 and detailed in Appendix A. The variability is not conveyed with the model configuration. Therefore, the sensible heat flux is not expected to decrease from Heat to Cool Square in reality. This assessment is overlooking a possible change in heat transfer coefficients from concrete to soil and traditional pavement.
The latent heat shows an increase of 100 % from Heat to Cool Square, with a 65% increase in vegetated area. This is likely explained by the transpiration rate of the turf grass and brush box tree in combination with the vertical character of the Brush Box trees. Turf grass has a typical leaf-specific plant hydraulic conductance of 1e-4 kg/(m².s.MPa), while the typical leaf-specific plant hydraulic conductance of the Brush Box tree is 1.4e-4 kg/(m².s.MPa) [12]. This explains, how the 0.4 % tree area on the Cool Square account for 35% of the latent heat increase compared to the Heat Square without trees. Leaf-specific plant hydraulic conductance values found in literature (see Table 3.2) suggest that the Elm, Red Beech, and Poplar tree species planted on the Cool Square in reality have similar transpiration rates. The Red Beech tree is factor five higher, the Poplar tree factor five lower, and the Elm tree similar to the model vegetation species. This suggests that the model output for plant transpiration is realistic, given the accurate representation of surrounding environmental conditions. The latent heat flux is calculated for transpiration, evaporation of canopy interception and soil evaporation per vegetation species based on size, structural and plant physiological characteristics, as well as soil water content and potential, surface temperature, and wind speed [12]. Note, the model calculation of plant transpiration is complex and dependent on several plant physiological factors as described in section 2.2.2. Hence, the discussed values can only give an indication. The grass species planted on the Cool Square is not known and likely a mix of different species as are the present shrubs. So, a specific comparison is difficult. However, the modelled and measured soil moisture below grass patches can give an indication if the modelled soil and grass evapotranspiration is realistic. The soil moisture values suggest a higher water availability and expected evapotranspiration rate for grass patches than modelled. A comparison of tree water availability cannot be made. Another influence is the model resolution limiting the accuracy of vegetation size. The grass and shrubs modelled as grass were given a height of zero meter, since the model has a maximum resolution of one meter. This is likely contributing to an underestimation of the latent heat flux as well.
The modelled ground heat flux of the Cool Square shows an increase over-topping the ground heat flux of the Heat Square, once the modelled evapotranspiration stopped. The modelled ground surface temperature does not show this trend and can therefore not be the driver of this heat flux occurrence. A potential explanation could be the vegetation surface temperature dependence on transpiration. Once this cooling mechanism stops and radiation influences are still present the vegetation surface temperature is likely to increase. Hence, the vegetation ground heat flux transported to the soil would also increase. However, the sensible heat flux does not show an increase at the same time. Therefore, it is more likely that evapotranspiration stopped because air temperature and surface temperature reached balance. Otherwise, the model output would suggest the depletion of available soil moisture for evapotranspiration. This is not the case. So, the increase in ground heat flux is likely due to an increase in soil moisture after soil moisture uptake for evapotranspiration stops. The increase in soil moisture reflects in an increased soil thermal conductivity and hence ground heat flux.

In summary, the sensible and ground heat flux for the Cool Square are expected to be higher than for the Heat Square in reality. The latent heat flux should also be higher, considering the differentiating vegetation size assumptions with VTUF-3D and simulated soil water availability.
Adding to the former recommendations, the vegetation characteristics of Elm, Poplar, and Red Beech tree

should be added to VTUF-3D and applied to fit the Cool Square tree species. Moreover, the initial soil moisture content and soil type characteristics should be fitted to the square characteristics. An analysis of the grass characteristics could also be useful. Additionally, an increase in possible model resolution is suggested to better represent vegetation size.

4.3.3 Wind Speed

Wind speed square averages are displayed in Figure 4.7. No change in modelled wind speed can be observed from the Heat to the Cool Square.

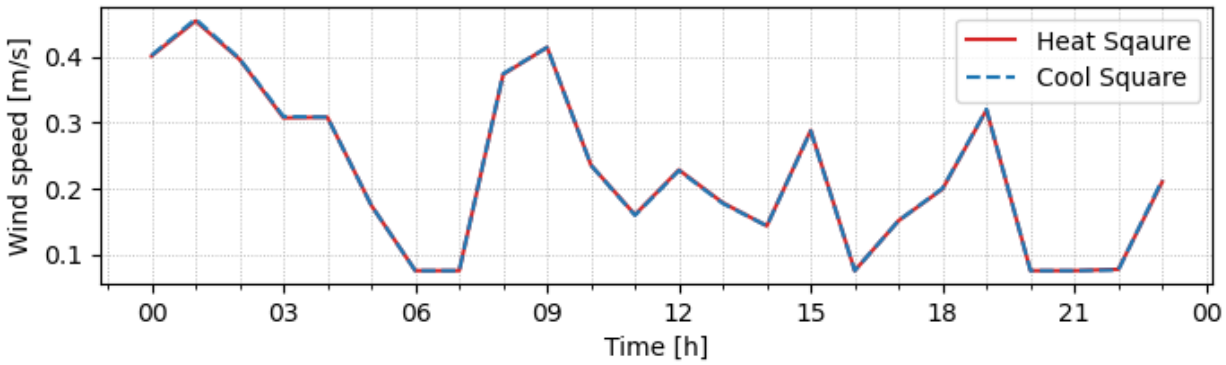

Figure 4.7: Wind speed time series simulation results for Heat and Cool Square. Results are square averages.

Modelled air flow does not show to change from Heat to Cool Square. This indicates that air flow, with its influence on the cooling effect, does not change with square configuration. However, the model bases air flow on geometrical arrangement and momentum roughness length, not air pressure differences [12]. Based on model momentum roughness lengths for grass, brush box, and road [12] the ground surface value drops by 9 %. This momentum roughness length does not appear to have a significant impact on the wind speed. The momentum roughness lengths for the square characteristics have not been measured. Hence an indication of the true roughness impact cannot be made. However, it is possible that air pressure differences increase from Heat to Cool Square and on the Cool Square itself, driving air flow. This is because of the different heating of the variable surfaces and the expected increase in humidity. This could mean a pressure difference from the square to the surrounding and boundary layer. So, a different air flow from Heat to Cool Square is expected, which the model cannot simulate. An additional factor for a future integration of pressure differences in air flow forcing may be the homogeneous area assumption of VTUF-3D around the study area [12]. Therefore, air pressure difference may not show as apparent as expected for a more variable neighbourhood.

In summary, the modelled wind speed does not show changes from Heat to Cool Square. The roughness effect assessment is lacking and potential air pressure effects cannot be modelled with the VTUF-3D equation for wind speed and the homogeneous area assumption in the model.
It is suggested to improve the model equation for wind speed and neighbourhood variability. Additionally, the roughness effect assessment should be updated with observations of square characteristics, on top of their integration in the model configuration.

4.3.4 Human Thermal Comfort

Figure 4.8 displays the UTCI distribution on the Heat Square (4.8a) and the Cool Square (4.8b) at 4 PM, the time of highest simulated UTCI values. Both square configurations show similar values per square characteristic. The area of road and building features shows a UTCI around 35, while areas with vegetation have a UTCI around 23. Hence, the Cool Square shows an increased area of UTCI equal to 23. A differentiation between vegetation types is not visible.

The UTCI values and distribution in Figure 4.8 show its relation to surface characteristics, see Figure 4.5. Vegetated surfaces appear to decrease the thermal stress given the model configuration. UTCI values from 9 to 26 indicate no thermal stress, values from 26 to 32 indicate moderate heat stress, values from 32 to 38 indicate strong heat stress, and values from 38 to 46 indicate very strong heat stress [71]. Hence, Figure4.8 suggests an increased area of no thermal stress compared to strong heat stress (UTCI $\bar{35}$) for the Cool Square, which is a great improvement in HTC. Given that the ground surface temperatures are expected to be different from the model output in reality (see section 4.1 and 4.2) the accuracy of the modelled UTCI is likely depreciated. Moreover, the UTCI calculation takes the relative humidity at the canopy level, which is not currently calculated with VTUF-3D. This limits the parameters significance. Furthermore, the wind speed speed is an influencing factor. So, as discussed above, modelled wind speed accuracy is likely different considering potential air pressure differences.

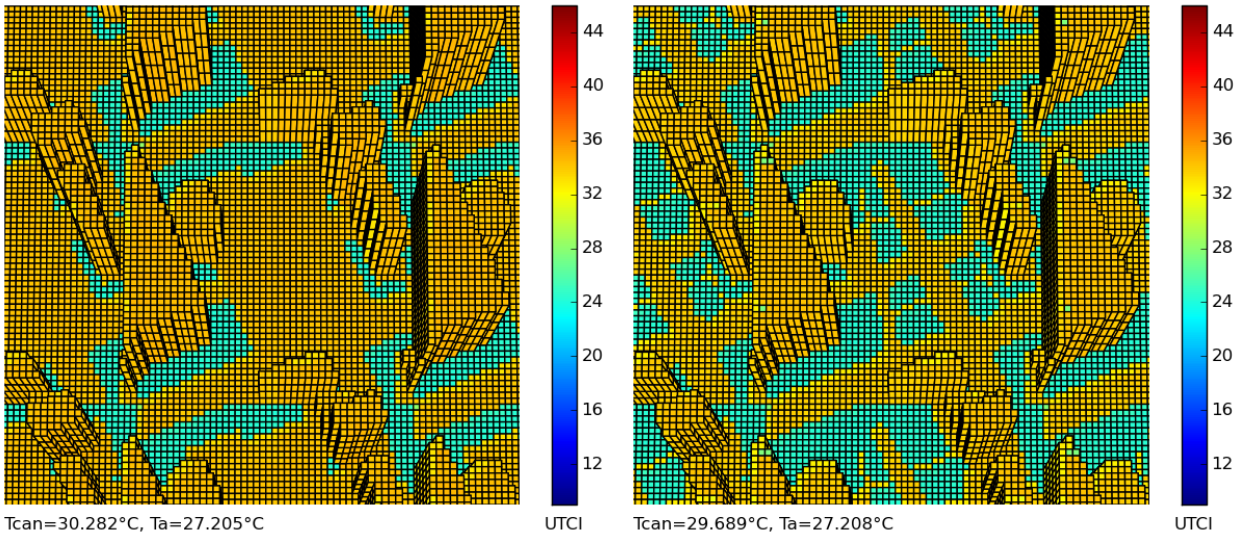

(a) Heat Square

(b) Cool Square

Figure 4.8: UTCI distribution for Heat (4.8a) and Cool Square (4.8b) at 4 PM. For reference, average canopy and air temperature values are indicated. Grid size is 1 m.

In summary, the modelled UTCI suggests a significant cooling effect through the added greening. However, the significance of the calculated UTCI is limited by the model parameter deviation from square characteristics affecting ground surface temperatures. Additionally, the UTCI calculation is lacking the modelled relative humidity and an updated wind speed simulation.
Therefore, the model configuration in its state does not give the expected greening effect on HTC. It is likely that an update of the fixed model parameters for the square characteristics gives more accurate results. However, for the HTC assessment the model requires an update of the UTCI calculation. Furthermore, refining the spatial analysis is recommended.

4.4 VTUF-3D Applicability

This sections aims to provide further considerations for the applicability of VTUF-3D. As argued before, VTUF-3D is an interesting model to assess the urban micro-climate at square scale with. It provides a detailed description of the water balance components in climate development, including detailed soil and plant physiological characteristics. As indicated in Appendix D, the model output is extensive and allows for climate impact assessment of the individual domain characteristic. The model code is publically available and free to add domain features, such as vegetation types and species.
As VTUF-3D is a recent development, from MAESPA and TUF-3D, and not a commercial model it lacks some user-friendliness. This limits the model in its potential. Hence, a further development is recommended. A first improvement can be made with the development of a comprehensive documentation covering most importantly the model scenario configuration with provided features and a detailed description of model output and its post-processing. Furthermore, the documentation can be extended to the model code for a better understanding of the model assumptions and calculations as well as possibilities for model extension in terms of domain features for assessment.
Additionally, it must be noted that the required software for the model is outdated since the model is developed on top of the older models TUF-3D and MAESPA, which is also reason for the combination and hence requirement of several programming languages. For applicability assurance in the future an update of the programming languages and required packages is recommended. Finally, simulations of longer time periods are possible but either take four hours per day or come with a decline in model accuracy (see Appendix B).

In summary, VTUF-3D is extensive in modelling the water balance with its components and its implications on the urban micro-climate. Advances should be made to enable the models full potential, especially considering user-friendliness.

5 Conclusion and Recommendations

How well can recent developments in urban micro-climate modelling predict the influence of greening on the micro-climate of urban squares? To answer this research question, a literature review on recent model developments was conducted. Additionally, a case study was performed for the Heat Square in the Green Village using the model VTUF-3D, chosen based on the literature review.

Five urban microclimate models exist that work on the integration of the water balance, namely **ENVI-met**, **i-Tree Hydro+**, **Solene-Microclimat**, **ST**, and **VTUF-3D**. No model describes a complete water balance. Mostly irrigation or evaporation from sealed surfaces is missing. Interestingly, parameters used to describe plant physiological characteristics vary per model. The models application is limited, depending on code availability, analysis options of nature-based solutions, and user-friendliness. Human Thermal Comfort (HTC) is only assessed by **ENVI-met** and **VTUF-3D**. Additionally, **ENVI-met** stands out for its comprehensive analysis options and user-friendliness. **VTUF-3D** is noticeable for its level of detail describing soil and plant characteristics. Note, the literature review is no holistic assessment and does not provide a conclusion on the overall performance of the models.

The case study simulation output suggests a significant cooling effect through heat mitigation via evapotranspiration and an increase in albedo. However, model output validation and the comparison of square characteristics with model feature parameters indicate that the model output deviates from the reality. The model feature parameters set in this investigation do not match with the measured square characteristics. Expected climate effects from Heat to Cool Square include an increase in ground surface temperature driven by a decrease in albedo. The sensible and ground heat flux are expected to increase, based on increased temperature gradients and estimated thermal capacity and conductance. VTUF-3D predicts an increase in latent heat flux, as expected. However, the latent heat flux is likely an underestimation, given the measured soil moisture deviation from model assumptions and model resolution limits. Further plant species specific effects remain to be investigated.
The simulation validation suggests a strong impact of the model feature parameters on the result accuracy. Given the detailed water balance simulation, it is expected that greening effects on the urban micro-climate of the Heat Square can be predicted accurately, when adjusting the model feature parameters to fit the square characteristics.

Four recommendations are given for further research, based on the literature review:

1. Further model development towards a comprehensive water balance representation and related analysis options,
2. Normalization efforts of soil and plant physiological parameterisation,
3. Establishment of a data base on plant species and characteristics to improve user-friendliness and present model users with several options for assessment,
4. Additional model validations for a wider range of environmental conditions.

Four recommendations are given for further research, based on the case study:

1. Development of a documentation for the use of VTUF-3D,
2. Improvement of model feature parameters to represent the Heat/Cool Square characteristics,
3. Model validation with heat flux measurements,
4. Improvement of UTCI prediction and spatial variability representation by VTUF-3D.

Efforts are taken to close the gap in urban micro-climate modelling considering the water balance integration. However, the studied models lack water balance components and need further validation and enhanced user-friendliness. Addressing these concerns will benefit the comprehensive and reliable evaluation of heat mitigation strategies in the context of climate change.

A Cool Square Design

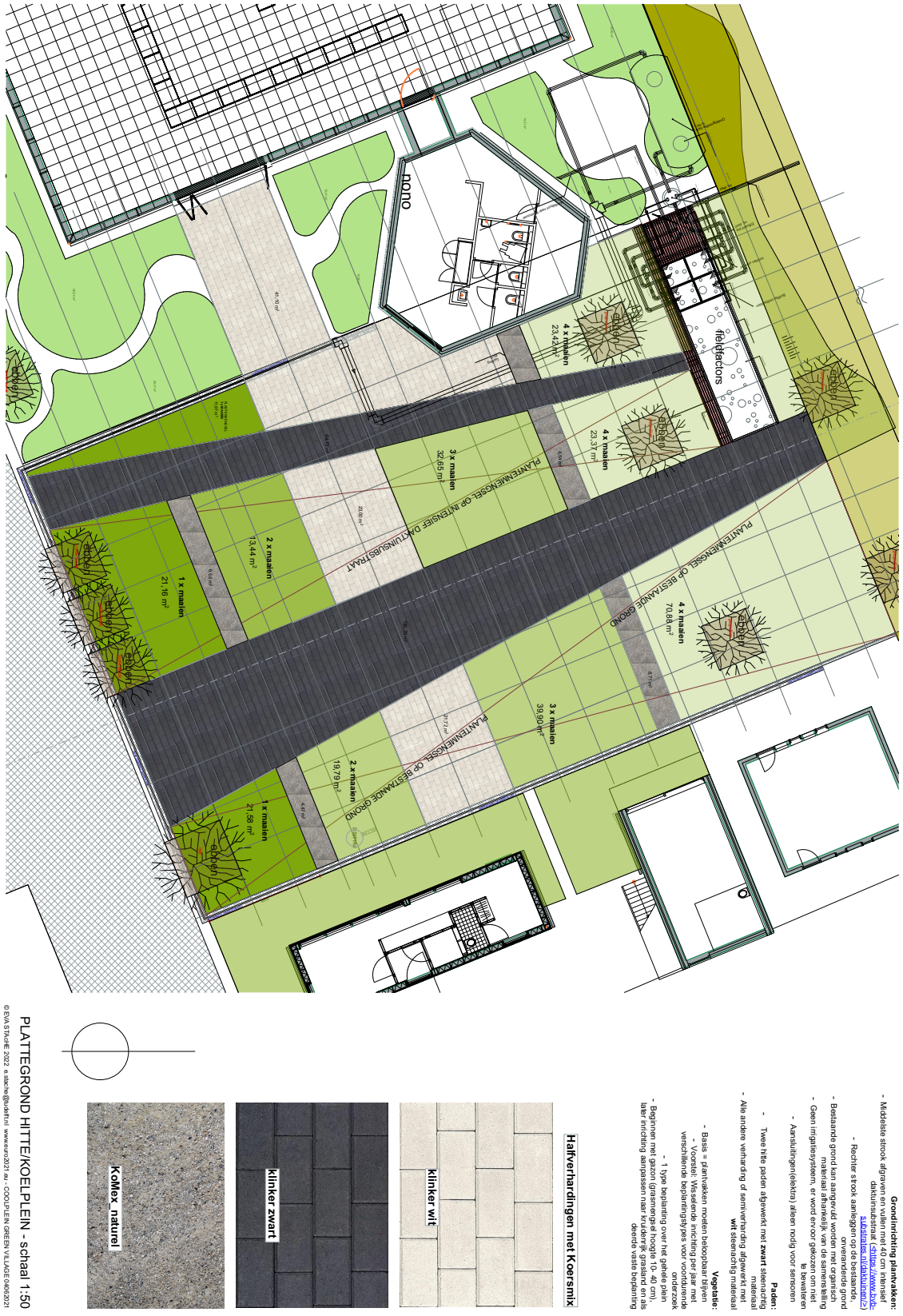

Figure A.1: Cool Square design by Eva Stache

B Fixed Model Parameters

B.1 TUF Model Parameters

```
1
204 999. 1.0 2022
10.0
T T F
0.001
0.15 0.10 0.30
0.92 0.92 0.88
0
1.0 0.123
0.5 4
0.020 1.20 1.75e6
0.020 1.20 1.75e6
0.010 0.03 0.10e6
0.030 1.50 2.25e6
0.020 0.80 2.00e6
0.030 0.80 2.00e6
0.100 0.90 1.50e6
0.500 0.30 1.25e6
0.020 1.10 1.75e6
0.030 1.10 2.00e6
0.090 1.10 2.00e6
0.020 0.30 1.50e6
-999. -999. -999.
0.05 0.05 -999. -999. 200. 1.0
4.31 6.0
2
18.0 23.0 22.0
22.0 20.0 19.0 15.0
0.01 0.01 0.01
52.0 0.01 52.0
1
0.31
1
1.5
```

```
** note: H/W of an individual canyon can be calculated by:
   H/W = sqrt(lpin)*bh_o_bl/(1-sqrt(lpin))  (ALTHOUGH, the model will
   increase the resolution if it is too low for any given facet, and
   this may result in the lambdap, bh_o_bl, or H/W ratios that you want
   not being met exactly
```

```
Parameters in the order that they are read in:

c model/integration parameters (further integration parameters are found
in the atmospheric forcing file (forcing.dat)
      read(299,*)vfcalc
      read(299,*)yd,deltat,outpt_tm,year,restart,restartTimestep
      read(299,*)Tthreshold
      read(299,*)facet_out,matlab_out,sum_out

c radiative parameters
      read(299,*)dalb
      read(299,*)albr,albs,albw
      read(299,*)emisr,emiss,emisw
      read(299,*)cloudtype

c conduction parameters
      read(299,*)IntCond,Intresist
      read(299,*)uc,numlayers
      do k=1,numlayers
       read(299,*)thickr(k),lambdar(k),htcapr(k)
      enddo
      do k=1,numlayers
       read(299,*)thicks(k),lambdas(k),htcaps(k)
      enddo
      do k=1,numlayers
       read(299,*)thickw(k),lambdaw(k),htcapw(k)
      enddo

c convection parameters
      read(299,*)z0,lambdaf,zrooffrc
      read(299,*)z0roofm,z0roadm,z0roofh,z0roadh,moh,rw

c domain geometry
      read(299,*)buildht_m,zref
      read(299,*)minres

c initial temperatures
      read(299,*)Tsfcr,Tsfcs,Tsfcw
      read(299,*)Tintw,Tints,Tfloor,Tbuild_min

c loop parameters
      read(299,*)stror_in,strorint,strormax
      read(299,*)xlat_in,xlatint,xlatmax
      read(299,*)numlp
      do k=1,numlp
       read(299,*)lpin(k)
      enddo
      read(299,*)numbhbl
      do l=1,numbhbl
       read(299,*)bh_o_bl(l)
      enddo


Explanation of the parameters:
```

```
* note: 'roads' and 'streets' are used interchangeably

c model/integration parameters
VFCALC: if vfcalc=0 (means no vf calcs) the file "vfinfo.dat" with
the correct view factor info must be in the run directory;
vfcalc=1 means exact plane parallel view factor calcs;
vfcalc=2 means contour integration view factor calcs; ** note: vfcalc
must be 1 or 2 if looping through lambdap is turned on (i.e. numlp>1)
YD: julian day (affects diurnal evolution of solar angle)
DELTAT: (seconds) input timestep - will be reduced by the model if needed
 - a large number (e.g. 999.) will ensure that the model controls the
timestep (recommended) - the model is optimized to find the largest
timestep (therefore the fastest run time) that is still stable at any
given time during the simulation
OUTPT_TM: (hours) how often model outputs are written
year: The year the simulation starts. If this is missing, the model defaults to 2004.
restart: New feature to allow restarted runs. If this is '1', it will restart at the restartTimestep.
restartTimestep: Which timestep to restart
TTHRESHOLD: (deg C) accuracy of Newton's method in solving the patch
energy balances - the smaller the number the higher the accuracy
FACET_OUT: 'T' = write out individual patch sky view factors, surface
temperatures, and absorbed/reflected solar radiation flux density,
organized by facet and location in the central urban unit;
'F' = do not write out these files
MATLAB_OUT: 'T' = write out files containing patch vertices and patch faces,
as well as patch surface temperature (Tsfc), patch brightness temperature
(Tbright), and patch net shortwave (Kstar); these three quantities can then
be easily visualized in Matlab with the 'patch' command; 'F' - do not write
these files
SUM_OUT: 'T' = write out individual patch surface temperatures (Tsfc) and
patch brightness temperature (Tbright) organized by TUF3D loop order (facet
direction varies slowest, then z, then y, then x) - so as to be easily read
in and assigned to the equivalent geometry (in the SUM model for example);
'F' = do not write out these files

c radiative parameters
DALB: (W/m2) accuracy to which the effective albedo/emissivity of the
canyon/cavity portion of the domain will be calculated; that is,
reflections will continue until the change in albedo between timesteps
is less than "dalb"
ALBR,ALBS,ALBW: albedo of roof, street, and wall patches, respectively
EMISR,EMISS,EMISW: emissivity of roof, street, and wall patches, respectively
CLOUDTYPE: For shortwave and longwave radiation; 0=clear, and higher values
(to a maximum of 7) are progressively thicker clouds; 1=cirrus, 2= cirrostratus,
3=altocumulus, 4=altostratus, 5=cumulonimbus, 6=stratocumulus, 7=thick stratus
(Ns?) - all assumed to be 100% cloud cover

c conduction parameters
INTCOND: 1=full conduction between deepest layer and ground/building
interior, 0=no such conduction...values between 0 and 1 are permitted
INTRESIST: resistance to energy exchange between deepest building layers
and building interior air (0.123 m2*K/W approximates combined conductive,
radiative, and convective exchange - Masson et al. 2002)
UC: degree of implicitness of solution of tridiagonal matrix for
conduction (1=fully implicit, 0=fully explicit, 0.5 is Crank-Nicholson and
is the most accurate, and is still stable - UC<0.5 may be unstable)
```

```
NUMLAYERS: number of layers for conduction in roofs, roads, walls
THICKR(k),LAMBDAR(k),HTCAPR(k): thickness (m), thermal conductivity
(W/m/K), and volumetric heat capacity (J/m3/K) of roof layer k, where k=1
is the surface layer, and k=numlayers is the deepest layer
THICKS(k),LAMBDAS(k),HTCAPS(k): same as for roofs, but for roads
THICKW(k),LAMBDAW(k),HTCAPW(k): same as for roofs, but for walls

**Note: the chosen conduction parameters put an upper limit on the model
time step for stability and accuracy reasons. If you want the model to run
faster, and it appears to be limited by its time step (i.e. time step is
below 20-30 seconds or so), then you may want to try making the solution
method more implicit (increase UC towards 1.0), or increasing the thickness
and heat capacity (or decreasing the thermal conductivity) of your thinnest
layers

c convection parameters
Z0: input town (i.e. overall) roughness length - model calculates it
according to Macdonald (1998) if values is less than 0
LAMBDAF: input town (i.e. overall) frontal area to plan area ratio
 - model calculates it if values is less than 0, and the model formula
depends on wind direction
ZROOFFRC: (m) the height above roof level for variables (temp, wind) used
to in forcing convection from roofs - model calculates it if the value
is negative
ZOROOFM,ZOROADM: (m) roof and road momentum roughness lengths, respectively
ZOROOFH,ZOROADH: (m) roof and road thermal roughness lengths, respectively
 - if values are negative model defaults to 1/200 of corresponding
momentum roughness lengths - **note that ratio of momentum to thermal
roughness lengths should never be smaller than 1/200! **
MOH: ratio of momentum to thermal roughness lengths for transfer from
individual *surfaces* only
RW: wall roughness relative to concrete (rw=1)

c domain geometry
BUILDHT_M: (m) height of buildings (mean height, if there is variation)
ZREF: (m) height of measured forcing data (air temperature, wind speed, etc)
 - must be greater than 'buildht_m'
MINRES: minimum resolution of any given facet (i.e. roof, road, or wall)
 - recommended value is 4 or greater (6 is ideal); resolution of all
other facets will be adjusted to maintain all geometric ratios while
ensuring that all facets have a minimum of 'minres' patches across them
in both dimensions (NOTE: THIS IS THE KEY PARAMETER THAT CONTROLS THE
ACCURACY OF THE RADIATION SCHEME VS. THE COMPUTATIONAL EXPENSE -
minres = 2 will give a quick estimate, minres = 4 tends to be a reasonable
balance between speed and accuracy, and minres = 6 tends to give very
accurate results but can be very computationally expensive and can require
a lot of memory, relative to the speed and memory of a typical desktop;
it is also useful to remember that the minimum resolution for solar
radiation absorption is effectively 2*minres - see the BLM paper for an
explanation)

c initial and constant temperatures
TSFCR,TSFCS,TSFCW: (deg C) initial surface temperatures (roofs, roads and
walls, respectively)
TINTW: (deg C) constant building internal air temperature (base of roofs
and walls)
```

```
TINTS: (deg C) constant deep-ground temperature (base of roads)
TFLOOR: (deg C) constant building internal floor temperature (affects
building internal temperature slightly)
TBUILD_MIN: (deg C) minimum indoor temperature permitted. If this
temperature is sufficiently high relative to the ambient temperature, it
will simulate space heating.

c loop parameters (for multiple simulations with the same forcing data,
but with different street orientations, latitudes, lambdap ratios, and
combinations thereof)
STROR_IN,STRORINT,STRORMAX: (degrees from alignment with cardinal
directions) initial, loop interval, and final street orientation
orientation
XLAT_IN,XLATINT,XLATMAX: (degrees) initial, loop interval, and final
latitude
NUMLP: number of lambdap ratios to loop through
LPIN(k): the lambdap ratios (from k=1 to k=numlp)
NUMBHBL: number of bh (building height) to bl (building width) ratios to
simulate for each lambdap
BH_O_BL(k): the bh/bl ratios (from l=1 to l=numbhbl)
```

B.2 Soil and Water Parameters for Turf Grass

```
&watcontrol
keepwet = 0 !Soil water stays wet if = 1 (used for testing)
simtsoil = 1 !Simulate soil temperature (yes=1) (must do)
simsoilevap = 1 !Simulate soil evaporation (yes=1)
reassignrain = 0 !Re-assign half hourly rain if only DAILY rainfall (PPT) available (yes=1)
wsoilmethod = 1 !If = 1 then use Emax method (unlimited water); if = 2 Use Vol Wat content;
if = 4 use exponenetial relationship with SMD1 & SMD2;
retfunction = 1 !Water retention curve (1=Campbell curve: parameters in "soilret")
equaluptake = 0 !water uptake from soil layers (0=based on fine root density and
soil water potential)
usemeaset = 0 !Use canopy transpiration if = 1; need to add 'ET' to met.dat file
usemeassw = 0 !Use measured soil water if = 1;
usestand = 0 !If = 1, water used by single trees scaled up to stand;
If=0, scaling not done - use for single tree in stand, or BY ITSELF
/

Rainfall canopy interception
&wattfall
rutterb = 3.7 !Drainage coefficient (B parameter in Rutter et al 1975) to
calculate canopy drainage (mm)
rutterd = 0.002 !Drainage parameter in Rutter et al 1975 (0.002) (dimensionless)
maxstorage = 0.4 !Maximum canopy storage of water
throughfall = 0.6 !rainfall passing through the canopy
/

&watinfilt
expinf = 0.0 !
/

Soil evaporation
```

```
&soiletpars
drythickmin = 0.01 !Minimum thickness of the dry soil layer (m)
tortpar = 0.66 !XX Parameter describing tortuosity of the soil: describes diffusion in porous media
/

Root parameters
&rootpars
rootrad = 0.0001 !Average root radius (m)
rootdens = 0.5e6 !Root density (g.m-3)
rootmasstot = 2.4 !Total root biomass (kg.m-2)
nrootlayer = 7 !Number of soil layers that are rooted. Together with the LAYTHICK parameter,
it determines the rooting depth
rootbeta = 0.9 !Beta parameter characterising root distribution (Jackson et al 1996)
/

Plant parameters
&plantpars
minrootwp = -2.5 !Minimum root water potential (MPa) (Fernandez and Moreno 2008)
minleafwp = -10 !Minimum leaf water potential (MPa) (not needed if MODELGS=6: Tuzet
model) (Giorio 1999)
plantk = 1.8 !leaf specific (total) plant hydraulic conductance (IMPORTANT!!!)
(Dichio et al 2013) (=3.21 kg.m-2.s-1.MPa-1 x 10^-5   divide by 1.8 x 10^-5 gives
1.8 mmol.m-2.s-1.MPa-1)
/

Soil water retention and conductivity (LOAM)
&soilret
bpar = 2.79 !Empiral coefficient related to clay content of the soil (Duusma et al. 2008)
psie = -0.00068 !air entry water potential (MPa) (LOAM) (Duursma et al. 2008)
ksat = 264.3 !saturated soil hydaulic conductivity (LOAM) (Duursma et al. 2008) (mol.m-1.s-1.MPa-1)
/

Soil layer parameters
&laypars
nlayer = 10 !number of soil layers in the model
laythick = 0.1 !Layer thickness (m)
porefrac = 0.38 !Soil porosity (m3.m-3)
Drainlimit = 0 !fraction of the pore fraction below which no drainage occurs (fraction 0-1)
fracorganic = 0 !Fraction of organic matter
/

Initial soil parameters
&initpars
initwater = 0.06 !Soil water content (m3.m-3)
soiltemp = 15 !Soil temperature
/
```

C VTUF-3D Input and Format

C.1 Meteorological Input from 23/07/2022

# Date	Time	SWdown	LWdown	Wind_E	Wind_N	PSurf	Tair	Qair	Rainf
2022-07-23	00:00:00	0.00	348.9	-0.527080	-0.249150	101700.0	289.35	0.094967	0.0
2022-07-23	00:30:00	0.00	344.1	-0.470064	0.317062	101700.0	289.25	0.093679	0.0
2022-07-23	01:00:00	0.00	361.2	0.525603	0.410646	101700.0	289.15	0.092846	0.0
2022-07-23	01:30:00	0.00	364.9	-0.423246	-0.197363	101700.0	289.05	0.093626	0.0
2022-07-23	02:00:00	0.00	346.7	-0.131193	-0.534124	101700.0	288.65	0.095179	0.0
2022-07-23	02:30:00	0.00	350.2	-0.000000	-0.467000	101700.0	288.55	0.098185	0.0
2022-07-23	03:00:00	0.00	346.2	-0.382865	-0.236462	101700.0	288.35	0.097867	0.0
2022-07-23	03:30:00	0.00	351.0	-0.482430	-0.264123	101700.0	288.25	0.096581	0.0
2022-07-23	04:00:00	0.00	353.4	-0.389711	-0.225000	101600.0	287.95	0.097854	0.0
2022-07-23	04:30:00	0.00	330.9	-0.118505	-0.451714	101700.0	287.75	0.096702	0.0
2022-07-23	05:00:00	0.00	329.0	-0.000000	-0.233000	101700.0	287.45	0.096550	0.0
2022-07-23	05:30:00	14.50	331.4	-0.000000	-0.000000	101700.0	287.65	0.098276	0.0
2022-07-23	06:00:00	24.80	327.9	-0.000000	-0.016700	101700.0	287.75	0.099424	0.0
2022-07-23	06:30:00	42.20	326.5	-0.000000	-0.233000	101700.0	288.45	0.099026	0.0
2022-07-23	07:00:00	98.80	344.3	-0.000000	-0.083300	101700.0	288.65	0.101675	0.0
2022-07-23	07:30:00	177.00	331.8	-0.000000	-0.167000	101700.0	290.75	0.101768	0.0
2022-07-23	08:00:00	232.00	331.0	-0.231978	-0.479870	101700.0	291.25	0.102120	0.0
2022-07-23	08:30:00	322.00	342.3	-0.256342	-0.348967	101700.0	291.55	0.101052	0.0
2022-07-23	09:00:00	310.00	333.9	-0.192690	-0.550236	101800.0	291.95	0.099262	0.0
2022-07-23	09:30:00	481.00	337.1	-0.120868	-0.451087	101800.0	293.35	0.100407	0.0
2022-07-23	10:00:00	593.00	360.2	-0.118251	-0.311297	101800.0	294.65	0.100407	0.0
2022-07-23	10:30:00	566.00	342.5	-0.013534	-0.232607	101800.0	294.95	0.095288	0.0
2022-07-23	11:00:00	765.00	350.2	-0.194966	-0.127582	101800.0	295.95	0.099279	0.0
2022-07-23	11:30:00	813.00	367.5	-0.027461	-0.348921	101800.0	296.75	0.104062	0.0
2022-07-23	12:00:00	876.00	361.4	-0.000000	-0.300000	101800.0	297.95	0.106369	0.0
2022-07-23	12:30:00	921.00	368.8	-0.116469	-0.434667	101800.0	297.95	0.104538	0.0
2022-07-23	13:00:00	958.00	382.5	-0.070167	-0.239951	101800.0	298.35	0.102683	0.0
2022-07-23	13:30:00	890.00	383.8	-0.000000	-0.150000	101800.0	299.65	0.103658	0.0
2022-07-23	14:00:00	709.00	381.0	-0.060141	-0.190743	101800.0	300.55	0.106908	0.0
2022-07-23	14:30:00	793.00	379.1	-0.153442	-0.153442	101800.0	300.65	0.111369	0.0
2022-07-23	15:00:00	756.00	386.1	-0.000000	-0.383000	101800.0	299.55	0.113380	0.0
2022-07-23	15:30:00	797.00	397.9	-0.349038	0.113409	101800.0	298.85	0.113577	0.0
2022-07-23	16:00:00	708.00	400.1	-0.000000	-0.083300	101700.0	300.35	0.107691	0.0
2022-07-23	16:30:00	679.00	400.1	-0.000000	-0.150000	101800.0	301.05	0.107791	0.0
2022-07-23	17:00:00	530.00	398.5	-0.000000	-0.200000	101700.0	300.15	0.100582	0.0
2022-07-23	17:30:00	504.00	399.3	-0.033076	-0.298171	101700.0	300.35	0.106478	0.0
2022-07-23	18:00:00	378.00	393.6	-0.000000	-0.267000	101700.0	298.85	0.103401	0.0
2022-07-23	18:30:00	349.00	392.7	-0.000000	-0.150000	101700.0	299.85	0.107863	0.0
2022-07-23	19:00:00	242.00	393.0	-0.426626	0.189946	101700.0	299.85	0.110230	0.0
2022-07-23	19:30:00	162.00	390.7	-0.073246	-0.273357	101700.0	298.45	0.110835	0.0
2022-07-23	20:00:00	80.40	387.0	-0.000000	-0.100000	101600.0	297.55	0.110094	0.0
2022-07-23	20:30:00	48.30	385.1	-0.000000	-0.066700	101600.0	297.25	0.109564	0.0
2022-07-23	21:00:00	32.50	379.4	-0.000000	-0.050000	101600.0	296.55	0.109116	0.0
2022-07-23	21:30:00	18.70	379.4	-0.000000	-0.066700	101700.0	295.55	0.110839	0.0
2022-07-23	22:00:00	3.83	373.2	-0.000000	-0.100000	101700.0	294.85	0.110226	0.0
2022-07-23	22:30:00	0.00	373.7	-0.000000	-0.250000	101700.0	294.55	0.107228	0.0
2022-07-23	23:00:00	0.00	369.1	-0.095191	-0.284497	101700.0	293.45	0.110014	0.0
2022-07-23	23:30:00	0.00	365.2	-0.000000	-0.100000	101700.0	293.15	0.112191	0.0

C.2 Meteorological Input from 13/06/2023

The meteorological input must be provided as CSV file in the following format:

# Date	Time	SWdown	LWdown	Wind_E	Wind_N	PSurf	Tair	Qair	Rainf
2023-06-12	23:00:00	0.000000	371.755920	-0.620558	-0.737774	101100.000000	295.300000	0.118617	0.0
2023-06-12	23:30:00	0.000000	369.572222	-0.620558	-0.737774	101100.000000	295.300000	0.118617	0.0
2023-06-13	00:00:00	0.000000	357.988222	-0.620558	-0.737774	101100.000000	295.300000	0.118617	0.0
2023-06-13	00:30:00	0.000000	357.130500	-0.290127	-0.499717	101150.000000	295.216667	0.103609	0.0
2023-06-13	01:00:00	0.000000	357.320389	-0.556636	-0.720809	101183.333333	295.166667	0.085469	0.0
2023-06-13	01:30:00	0.000000	352.658500	-0.372443	-0.630500	101200.000000	295.000000	0.081574	0.0
2023-06-13	02:00:00	0.000000	348.755889	-0.262338	-0.367663	101183.333333	294.466667	0.078981	0.0
2023-06-13	02:30:00	0.000000	345.520833	-0.352565	-0.603799	101116.666667	293.933333	0.077140	0.0
2023-06-13	03:00:00	0.372850	343.243222	-0.061929	-0.522428	101100.000000	293.516667	0.075701	0.0
2023-06-13	03:30:00	7.058378	341.237000	-0.102610	-0.431335	101100.000000	293.083333	0.074679	0.0
2023-06-13	04:00:00	16.340344	340.138056	-0.236320	-0.496056	101100.000000	292.516667	0.073957	0.0
2023-06-13	04:30:00	23.645400	339.865556	-0.270955	-0.587371	101100.000000	292.050000	0.073741	0.0
2023-06-13	05:00:00	31.265606	339.658722	-0.646000	-0.736065	101100.000000	291.483333	0.072863	0.0
2023-06-13	05:30:00	44.861350	342.168444	-0.531646	-0.439472	101100.000000	291.050000	0.073220	0.0
2023-06-13	06:00:00	64.973800	345.568167	-0.276575	-0.637866	101100.000000	291.300000	0.074848	0.0
2023-06-13	06:30:00	62.849867	352.431667	-0.566264	-0.742473	101166.666667	291.833333	0.076256	0.0
2023-06-13	07:00:00	224.736739	354.178222	-0.439369	-0.692366	101200.000000	291.900000	0.077904	0.0
2023-06-13	07:30:00	265.123028	356.900000	-0.634430	-0.833700	101200.000000	292.366667	0.078853	0.0
2023-06-13	08:00:00	580.787167	361.804000	-0.287839	-0.743398	101200.000000	293.216667	0.081709	0.0
2023-06-13	08:30:00	586.269778	364.420833	-0.359387	-0.492431	101200.000000	294.616667	0.085088	0.0
2023-06-13	09:00:00	707.103889	374.624722	-0.525524	-0.559942	101216.666667	296.466667	0.083687	0.0
2023-06-13	09:30:00	756.814944	376.571833	-0.434487	-0.314361	101300.000000	297.700000	0.083619	0.0
2023-06-13	10:00:00	792.479889	379.324167	-0.757150	-0.453392	101300.000000	298.600000	0.081280	0.0
2023-06-13	10:30:00	821.818889	381.987167	-0.762060	-0.644698	101300.000000	298.950000	0.078686	0.0
2023-06-13	11:00:00	844.068333	383.630111	-1.190256	-0.639780	101200.000000	299.283333	0.075673	0.0
2023-06-13	11:30:00	849.137778	386.038222	-1.137698	-0.472737	101200.000000	300.016667	0.073541	0.0
2023-06-13	12:00:00	839.325556	388.349833	-0.773324	-0.903394	101200.000000	299.616667	0.072714	0.0
2023-06-13	12:30:00	834.358333	389.096611	-0.603040	-0.718841	101200.000000	300.033333	0.071885	0.0
2023-06-13	13:00:00	811.452889	389.837556	-0.590815	-0.923970	101200.000000	300.433333	0.072302	0.0
2023-06-13	13:30:00	765.406889	393.066944	-1.198102	-0.975340	101200.000000	300.466667	0.071961	0.0
2023-06-13	14:00:00	715.490222	391.808222	-0.537761	-0.445639	101200.000000	301.166667	0.075561	0.0
2023-06-13	14:30:00	661.036500	390.350111	-0.945370	-0.402033	101200.000000	302.600000	0.078936	0.0
2023-06-13	15:00:00	596.597278	388.427333	-1.039999	-0.766981	101133.333333	301.666667	0.076589	0.0
2023-06-13	15:30:00	531.723056	386.951500	-0.136960	-0.383030	101100.000000	301.983333	0.079634	0.0
2023-06-13	16:00:00	470.036667	384.866889	-0.196385	-1.161223	101100.000000	301.266667	0.078573	0.0
2023-06-13	16:30:00	398.703278	382.247111	-0.357399	-1.389892	101100.000000	300.400000	0.076509	0.0
2023-06-13	17:00:00	321.635778	378.366333	-0.305756	-1.387712	101100.000000	300.483333	0.074121	0.0
2023-06-13	17:30:00	242.285056	375.583889	-0.323086	-1.219309	101100.000000	300.400000	0.073065	0.0
2023-06-13	18:00:00	169.690667	372.647889	-0.452670	-1.057446	101050.000000	300.516667	0.071884	0.0
2023-06-13	18:30:00	98.628522	369.502722	-0.367701	-1.406202	101000.000000	299.833333	0.075621	0.0
2023-06-13	19:00:00	29.378856	365.172278	-0.225936	-1.269886	101033.333333	299.066667	0.078685	0.0
2023-06-13	19:30:00	7.826083	361.702556	-0.195453	-1.546144	101050.000000	298.750000	0.082051	0.0
2023-06-13	20:00:00	0.000000	358.296889	-0.247803	-1.600744	101083.333333	298.083333	0.088834	0.0
2023-06-13	20:30:00	0.000000	355.891778	-0.392680	-1.145365	101100.000000	297.466667	0.096999	0.0
2023-06-13	21:00:00	0.000000	354.246000	-0.248501	-1.563107	101100.000000	296.616667	0.098144	0.0
2023-06-13	21:30:00	0.000000	352.014889	-0.454173	-0.872414	101100.000000	295.833333	0.096273	0.0
2023-06-13	22:00:00	0.000000	349.992167	-0.149287	-1.384435	101116.666667	295.200000	0.094474	0.0
2023-06-13	22:30:00	0.000000	348.204889	-0.073521	-1.420287	101200.000000	294.750000	0.095677	0.0
2023-06-13	23:00:00	0.000000	347.500000	-0.157822	-0.858792	101200.000000	294.350000	0.095414	0.0
2023-06-13	23:30:00	0.000000	347.500000	-0.074559	-1.010538	101200.000000	294.150000	0.089994	0.0

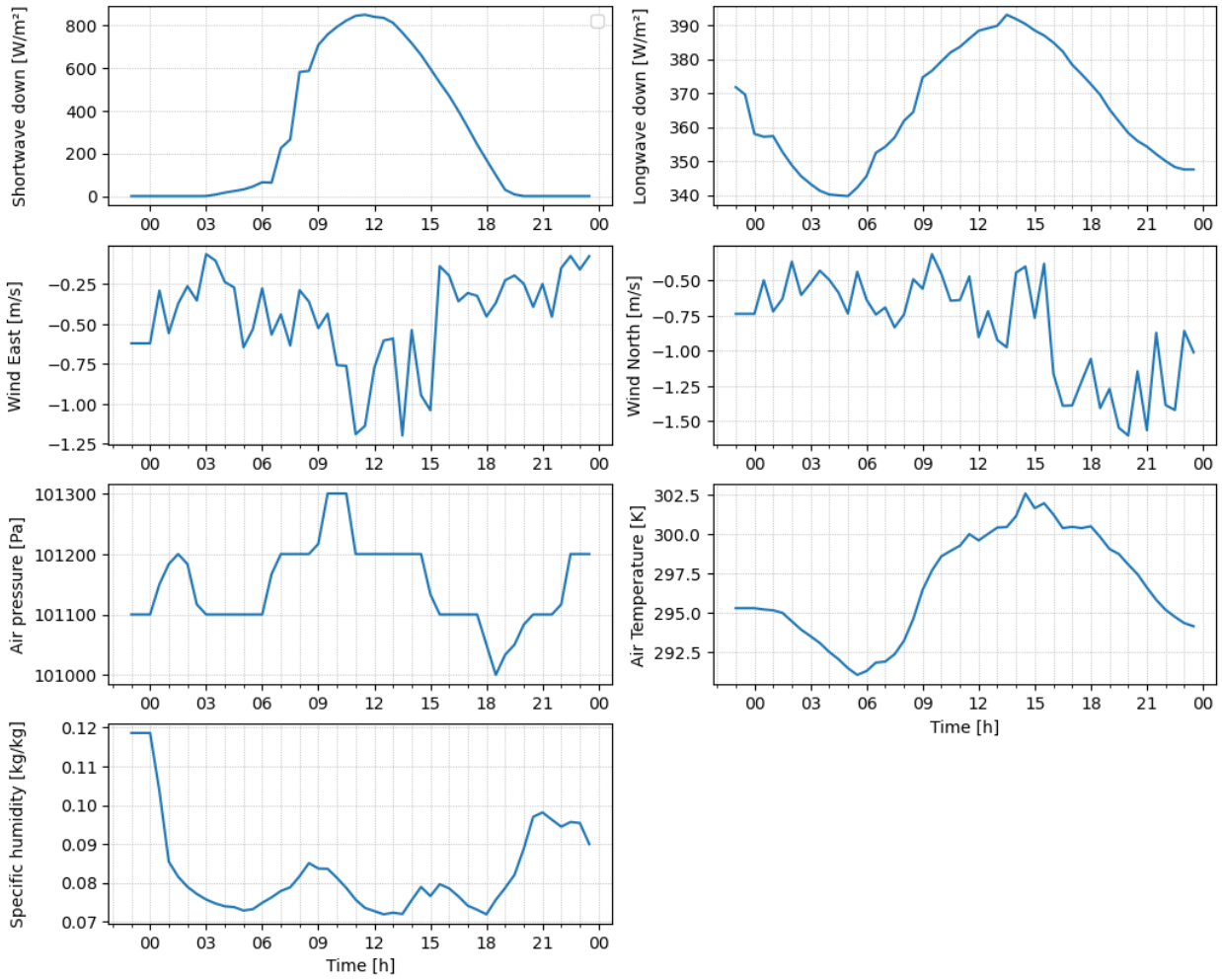

Figure C.1: Meteorological forcing data 13/06/2023

C.3 Domain Configuration Format

The domain configuration is provided to the model as CSV files, one file per domain attribute. The values in the CSV file must be organized according to the grid patch location and must show the following format:

”0” ”0” ”0”
”0” ”0” ”0”
”0” ”0” ”0”

D Model Output

VTUF-3D outputs several files of hourly time series data for the simulated date(s). The output files and parameters are summarized below.

file **EnergyBalance_Overall.out** gives square average data for the energy balance components per square characteristics. Parameters include:

```
lambdap,H/L,H/W,latitude,streetdir,julian_day,time_of_day,time(continuous),Rnet_tot,Qh_SumSfc,Qh_Vol,
Qg_SumSfc,Qg_SfcCanAir,Rnet_can,Qh_CanTop,Qh_SumCanSfc,Qg_Can_CanAir,Ucan,Utop,Uroad,wstar,Kdn,Kup,
Ldn,Lup,Kdir_Calc,Kdif_Calc,Kdir,Kdif,Kup_can,Lup_can,az,zen,Kdn(NoAtm),Kdn_grid,Qe_tot
```

file **EnergyBalance_Facets.out** gives heat fluxes per facet orientation. Parameters include:

```
lambdap,H/L,H/W,latitude,streetdir,julian_day,time_of_day,time(continuous),QR,HR,GR,QT,HT,GT,QN,HN,
GN,QS,HS,GS,QE,HE,GE,QW,HW,GW
```

file **RadiationBalance_Facets.out** gives shortwave and longwave radiation per facet orientation:

```
lambdap,H/L,H/W,latitude,streetdir,julian_day,time_of_day,time(continuous),SKd,SKup,SLd,SLup,EKd,
EKup,ELd,ELup,NKd,NKup,NLd,NLup,WKd,WKup,WLd,WLup,RfKd,RfKup,RfLd,RfLup,FKd,FKup,FLd,FLup
```

file **EnergyBalance_Tsfc_TimeAverage.out** gives square averages for radiation and heat fluxes as well as facet temperatures per orientation:

```
lambdap,H/L,H/W,latitude,streetdir,julian_day,time_of_day(centre),time(continuous&centre),
time_of_day(end),time(continuous&end),Kuptot_avg,Luptot_avg,Rntot_avg,Qhtot_avg,Qgtot_avg,
Qanthro_avg,Qac_avg,Qdeep_avg,Qtau,TR_avg,TT_avg,TN_avg,TS_avg,TE_avg,TW_avg
```

file **Tsfc_Facets.out** gives various surface temperatures (per orientation/lighting/property), the average canyon air temperature, and heat capacity of roof, wall, and ground:

```
lambdap,H/L,H/W,latitude,streetdir,julian_day,time_of_day,time(continuous),Tcomplete,Tbirdeye,
Troof,Troad,Tnorth,Tsouth,Teast,Twest,Tcan,Ta,Tint,httcR,httcT,httcW,TbrightR,TbrightT,TbrightN,
TbrightS,TbrightE,TbrightW
```

file **watbal.dat** additionally gives the following half-hourly parameters per vegetation species:

```
Half-hourly water and heat balance components.
wsoil: total soil water storage                      mm
wsoilroot: soil water storage in rooted zone         mm
ppt : precipitation                                  mm
canopystore : storage of intercepted rain            mm
evapstore : evaporation of wet canopy                mm
drainstore : drainage of wet canopy                  mm
tfall : throughfall of rain                          mm
et : modelled canopy transpiration                   mm
etmeas: measured ET, if provided in input            mm
discharge: drainage at bottom of profile             mm
overflow: over-land flow                             mm
weightedswp: soil water potential weighted by roots  MPa
```

```
ktot: soil to leaf hydr. cond.        mmol m-2 s-1 MPa-1
drythick: thickness of dry surface layer              mm
soilevap: soil evaporation                            mm
soilmoist: measured soil water content      (units vary)
fsoil: soil water modifier function                (0-1)
qh: sensible heat flux                             W m-2
qe: latent heat flux                               W m-2
qn: net radiation                                  W m-2
qc: soil heat transport                            W m-2
rglobund: net radiation underneath canopy          W m-2
rglobabv: net radiation above canopy               W m-2
radinterc: total radiation intercepted by canopy   W m-2
rnet: net radiation above the canopy               W m-2
totlai: leaf area index                           m2 m-2
tair: air temperature                              deg C
soilt1, soilt2: soil T in 1st and 2nd layer        deg C
fracw1,fracw2: water content 1st and 2nd layer    m3 m-3
FracaPAR: fraction of absorbed PAR
'''
```

file **hrflux.dat** gives data on soil and plant physiological parameters:

```
    hrPAR: absorbed PAR              umol tree-1 s-1
hrNIR: absorbed NIR              W tree-1
hrTHM: absorbed thermal          W tree-1
hrPS: photosynthesis (net of leaf resp) umol tree-1 s-1
hrRf:  hourly leaf respiration   umol tree-1 s-1
hrRmW: hourly stem + branch Rm   umol tree-1 s-1
hrLE:  hourly transpiration      mmol tree-1 s-1
LECAN: hourly transpirn: CANOPY calc : mmol H2O m-2 s-1
Gscan: canopy stomatal conductance : mol CO2 tree-1 s-1
Gbhcan: canopy boundary layer conductance to heat : mol tree-1 s-1
hrH:   hourly sensible heat flux:  MJ tree-1 s-1
TCAN: Average foliage temperature (deg C)
ALMAX: Canopy maximum leaf photosynthesis rate (umol m-2 s-1)
PSIL: Canopy average leaf water potential (MPa)
PSILMIN: Canopy minimum leaf water potential (MPa)
CI : Canopy average intercellular CO2 conc. (ppm)
TAIR: Air temperature (deg C)
VPD: vapor pressure deficit (kPa)
PAR: Above-canopy incident PAR (umol m-2 s-1)
ZEN: Zenithal angle (rad)
AZ: Asimutal angle (rad)
```

References

[1] Timothy R Oke, Gerald Mills, Andreas Christen, and James A Voogt. *Urban climates*. Cambridge University Press, 2017.

[2] Jane Wilson Baldwin, Jay Benjamin Dessy, Gabriel A. Vecchi, and Michael Oppenheimer. Temporally Compound Heat Wave Events and Global Warming: An Emerging Hazard. *Earth's Future*, 7(4):411–427, April 2019.

[3] S. E. Perkins, L. V. Alexander, and J. R. Nairn. Increasing frequency, intensity and duration of observed global heatwaves and warm spells. *Geophysical Research Letters*, 39(20):2012GL053361, October 2012.

[4] Miklós Székely, Luís Carletto, and András Garami. The pathophysiology of heat exposure. *Temperature*, 2(4):452–452, October 2015.

[5] Belén Sanz-Barbero, Cristina Linares, Carmen Vives-Cases, José Luis González, Juan José López-Ossorio, and Julio Díaz. Heat wave and the risk of intimate partner violence. *Science of The Total Environment*, 644:413–419, December 2018.

[6] Barry S. Levy, Victor W. Sidel, and Jonathan A. Patz. Climate Change and Collective Violence. *Annual Review of Public Health*, 38(1):241–257, March 2017.

[7] Jean-Marie Robine, Siu Lan K. Cheung, Sophie Le Roy, Herman Van Oyen, Clare Griffiths, Jean-Pierre Michel, and François Richard Herrmann. Death toll exceeded 70,000 in Europe during the summer of 2003. *Comptes Rendus Biologies*, 331(2):171–178, February 2008.

[8] Joan Ballester, Marcos Quijal-Zamorano, Raúl Fernando Méndez Turrubiates, Ferran Pegenaute, François R Herrmann, Jean Marie Robine, Xavier Basagaña, Cathryn Tonne, Josep M Antó, and Hicham Achebak. Heat-related mortality in europe during the summer of 2022. *Nature medicine*, pages 1–10, 2023.

[9] Yuming Guo, Antonio Gasparrini, Shanshan Li, Francesco Sera, Ana Maria Vicedo-Cabrera, Micheline de Sousa Zanotti Stagliorio Coelho, Paulo Hilario Nascimento Saldiva, Eric Lavigne, Benjawan Tawatsupa, Kornwipa Punnasiri, Ala Overcenco, Patricia Matus Correa, Nicolas Valdes Ortega, Haidong Kan, Samuel Osorio, Jouni J. K. Jaakkola, Niilo R. I. Ryti, Patrick G. Goodman, Ariana Zeka, Paola Michelozzi, Matteo Scortichini, Masahiro Hashizume, Yasushi Honda, Xerxes Seposo, Ho Kim, Aurelio Tobias, Carmen Íñiguez, Bertil Forsberg, Daniel Oudin Åström, Yue Leon Guo, Bing-Yu Chen, Antonella Zanobetti, Joel Schwartz, Tran Ngoc Dang, Dung Do Van, Michelle L. Bell, Ben Armstrong, Kristie L. Ebi, and Shilu Tong. Quantifying excess deaths related to heatwaves under climate change scenarios: A multicountry time series modelling study. *PLOS Medicine*, 15(7):e1002629, July 2018.

[10] Fernando Pacheco Torgal, J. Labrincha, Luisa F. Cabeza, and Claes G. Granqvist, editors. *Eco-efficient materials for mitigating building cooling needs: design, properties and applications*. Number Number 56 in Woodhead Publishing series in civil and structural engineering. Woodhead Publishing, Cambridge, 2015. OCLC: ocn907283288.

[11] Krzysztof Blazejczyk, Yoram Epstein, Gerd Jendritzky, Henning Staiger, and Birger Tinz. Comparison of utci to selected thermal indices. *International journal of biometeorology*, 56:515–535, 2012.

[12] Kerry Nice. *Development, validation, and demonstration of the VTUF-3D v1.0 urban micro-climate model to support assessments of urban vegetation influences on human thermal comfort*. PhD thesis, Monash University, 2016.

[13] Pninit Cohen, Oded Potchter, and Andreas Matzarakis. Daily and seasonal climatic conditions of green urban open spaces in the mediterranean climate and their impact on human comfort. *Building and environment*, 51:285–295, 2012.

[14] Hyunjung Lee, Jutta Holst, Helmut Mayer, et al. Modification of human-biometeorologically significant radiant flux densities by shading as local method to mitigate heat stress in summer within urban street canyons. *Advances in Meteorology*, 2013, 2013.

[15] Ferdinand Briegel, Jonas Wehrle, Dirk Schindler, and Andreas Christen. High-resolution multi-scaling of outdoor human thermal comfort and its intra-urban variability based on machine learning. *Geoscientific Model Development Discussions*, 2023:1–31, 2023.

[16] Pamela Smith, Pablo Sarricolea, Orlando Peralta, Juan Pablo Aguila, and Felipe Thomas. Study of the urban microclimate using thermal uav. the case of the mid-sized cities of arica (arid) and curicó (mediterranean), chile. *Building and Environment*, 206:108372, 2021.

[17] Briony A. Norton, Andrew M. Coutts, Stephen J. Livesley, Richard J. Harris, Annie M. Hunter, and Nicholas S.G. Williams. Planning for cooler cities: A framework to prioritise green infrastructure to mitigate high temperatures in urban landscapes. *Landscape and Urban Planning*, 134:127–138, February 2015.

[18] Tobi Eniolu Morakinyo, Ling Kong, Kevin Ka-Lun Lau, Chao Yuan, and Edward Ng. A study on the impact of shadow-cast and tree species on in-canyon and neighborhood's thermal comfort. *Building and Environment*, 115:1–17, 2017.

[19] Mohammad A Rahman, Laura MF Stratopoulos, Astrid Moser-Reischl, Teresa Zölch, Karl-Heinz Häberle, Thomas Rötzer, Hans Pretzsch, and Stephan Pauleit. Traits of trees for cooling urban heat islands: A meta-analysis. *Building and Environment*, 170:106606, 2020.

[20] Teresa Zölch, Johannes Maderspacher, Christine Wamsler, and Stephan Pauleit. Using green infrastructure for urban climate-proofing: An evaluation of heat mitigation measures at the micro-scale. *Urban Forestry & Urban Greening*, 20:305–316, December 2016.

[21] Rocco Pace, Francesco De Fino, Mohammad A. Rahman, Stephan Pauleit, David J. Nowak, and Rüdiger Grote. A single tree model to consistently simulate cooling, shading, and pollution uptake of urban trees. *International Journal of Biometeorology*, 65(2):277–289, February 2021. 7.

[22] Adam Berland, Sheri A Shiflett, William D Shuster, Ahjond S Garmestani, Haynes C Goddard, Dustin L Herrmann, and Matthew E Hopton. The role of trees in urban stormwater management. *Landscape and urban planning*, 162:167–177, 2017.

[23] Nancy B Grimm, Stanley H Faeth, Nancy E Golubiewski, Charles L Redman, Jianguo Wu, Xuemei Bai, and John M Briggs. Global change and the ecology of cities. *science*, 319(5864):756–760, 2008.

[24] Jennifer A Salmond, Marc Tadaki, Sotiris Vardoulakis, Katherine Arbuthnott, Andrew Coutts, Matthias Demuzere, Kim N Dirks, Clare Heaviside, Shanon Lim, Helen Macintyre, et al. Health and climate related ecosystem services provided by street trees in the urban environment. *Environmental Health*, 15(1):95–111, 2016.

[25] Kheng Siang Ted Ng, Angelia Sia, Maxel KW Ng, Crystal TY Tan, Hui Yu Chan, Chay Hoon Tan, Iris Rawtaer, Lei Feng, Rathi Mahendran, Anis Larbi, et al. Effects of horticultural therapy on asian older adults: A randomized controlled trial. *International journal of environmental research and public health*, 15(8):1705, 2018.

[26] Mohammad A Rahman, Astrid Moser, Anna Gold, Thomas Rötzer, and Stephan Pauleit. Vertical air temperature gradients under the shade of two contrasting urban tree species during different types of summer days. *Science of the Total Environment*, 633:100–111, 2018.

[27] Cho Kwong Charlie Lam, Hyunjung Lee, Shing-Ru Yang, and Sookuk Park. A review on the significance and perspective of the numerical simulations of outdoor thermal environment. *Sustainable Cities and Society*, 71:102971, August 2021. 2.

[28] Bhaswati Ray and S Rajib. *Urban Drought*. Springer, 2019.

[29] Xiang Zhang, Nengcheng Chen, Hao Sheng, Chris Ip, Long Yang, Yiqun Chen, Ziqin Sang, Tsegaye Tadesse, Tania Pei Yee Lim, Abbas Rajabifard, et al. Urban drought challenge to 2030 sustainable development goals. *Science of the Total Environment*, 693:133536, 2019.

[30] Beena Balan Sarojini, Peter A Stott, and Emily Black. Detection and attribution of human influence on regional precipitation. *Nature Climate Change*, 6(7):669–675, 2016.

[31] Y. Toparlar, B. Blocken, B. Maiheu, and G.J.F. van Heijst. A review on the CFD analysis of urban microclimate. *Renewable and Sustainable Energy Reviews*, 80:1613–1640, December 2017.

[32] Timothé Robineau, Auline Rodler, Benjamin Morille, David Ramier, Jérémie Sage, Marjorie Musy, Vincent Graffin, and Emmanuel Berthier. Coupling hydrological and microclimate models to simulate evapotranspiration from urban green areas and air temperature at the district scale. *Urban Climate*, 44:101179, July 2022.

[33] Implications of Thermodynamics for Sustainability. In Heriberto Cabezas and Urmila Diwekar, editors, *Sustainability: Multi-Disciplinary Perspectives*, pages 222–242. BENTHAM SCIENCE PUBLISHERS, September 2012.

[34] Naika Meili, Gabriele Manoli, Paolo Burlando, Jan Carmeliet, Winston T.L. Chow, Andrew M. Coutts, Matthias Roth, Erik Velasco, Enrique R. Vivoni, and Simone Fatichi. Tree effects on urban microclimate: Diurnal, seasonal, and climatic temperature differences explained by separating radiation, evapotranspiration, and roughness effects. *Urban Forestry & Urban Greening*, 58:126970, March 2021. 9 linked.

[35] Zheng Tan, Kevin Ka-Lun Lau, and Edward Ng. Urban tree design approaches for mitigating daytime urban heat island effects in a high-density urban environment. *Energy and Buildings*, 114:265–274, 2016.

[36] Nicole Müller, Wilhelm Kuttler, and Andreas-Bent Barlag. Counteracting urban climate change: adaptation measures and their effect on thermal comfort. *Theoretical and applied climatology*, 115:243–257, 2014.

[37] Petra Hesslerová, Jan Pokorný, Hanna Huryna, Josef Seják, and Vladimír Jirka. The impacts of greenery on urban climate and the options for use of thermal data in urban areas. *Progress in Planning*, 159:100545, May 2022.

[38] Andrew Gettelman and Richard B. Rood. Essence of a Climate Model. In *Demystifying Climate Models*, volume 2, pages 37–58. Springer Berlin Heidelberg, Berlin, Heidelberg, 2016. Series Title: Earth Systems Data and Models.

[39] Ruibin Li, Zhanpeng Liu, Lu Feng, and Naiping Gao. Fast fluid dynamics simulation of the airflow distributions in urban residential areas. *Energy and Buildings*, 255:111635, January 2022.

[40] Jianxiang Huang, Tongping Hao, Yali Wang, and Phil Jones. A street-scale simulation model for the cooling performance of urban greenery: Evidence from a high-density city. *Sustainable Cities and Society*, 82:103908, July 2022. 8.

[41] P.J.C. Schrijvers. *Urban Climate at Street Scale: Analysis and Adaptation*. PhD thesis, Delft University of Technology, 2020. 4.

[42] Cezary Sławiński and Henryk Sobczuk. Soil–Plant–Atmosphere Continuum. In Jan Gliński, Józef Horabik, and Jerzy Lipiec, editors, *Encyclopedia of Agrophysics*, Encyclopedia of Earth Sciences Series, pages 805–810. Springer Netherlands, Dordrecht, 2011.

[43] Stefano Leonardi, Paolo Piovani, Federico Magnani, and Paolo Menozzi. A simple general method to evaluate intra-specific transpiration parameters within and among seedling families. *Oecologia*, 149(2):185–193, August 2006.

[44] Mohammad A. Rahman, Astrid Moser, Thomas Rötzer, and Stephan Pauleit. Microclimatic differences and their influence on transpirational cooling of Tilia cordata in two contrasting street canyons in Munich, Germany. *Agricultural and Forest Meteorology*, 232:443–456, January 2017. 7 linked.

[45] Xiuhua Zhao, Ping Zhao, Liuwei Zhu, Qian Wang, Yanting Hu, Benjamin M. Cranston, Julia Kaplick, Ouyang Lei, Xia Chen, Guangyan Ni, Qing Ye, and Cate Macinnis-Ng. Exploring the Influence of Biological Traits and Environmental Drivers on Water Use Variations across Contrasting Forests. *Forests*, 12(2):161, January 2021.

[46] Christiane Weber. Ecosystem services provided by urban vegetation: a literature review. In *Urban Environment: Proceedings of the 11th Urban Environment Symposium (UES), held in Karlsruhe, Germany, 16-19 September 2012*, pages 119–131. Springer, 2013.

[47] Zhixin Liu, Wenwen Cheng, C.Y. Jim, Tobi Eniolu Morakinyo, Yuan Shi, and Edward Ng. Heat mitigation benefits of urban green and blue infrastructures: A systematic review of modeling techniques, validation and scenario simulation in ENVI-met V4. *Building and Environment*, 200:107939, August 2021.

[48] Yang Yang, Theodore A. Endreny, and David J. Nowak. A physically based analytical spatial air temperature and humidity model. *Journal of Geophysical Research: Atmospheres*, 118(18):10,449–10,463, September 2013. 13.

[49] Jun Wang, Theodore A. Endreny, and David J. Nowak. Mechanistic Simulation of Tree Effects in an Urban Water Balance Model. *JAWRA Journal of the American Water Resources Association*, 44(1):75–85, February 2008. 13.2.

[50] Satoshi Hirabayashi, Charles N. Kroll, and David J. Nowak. Component-based development and sensitivity analyses of an air pollutant dry deposition model. *Environmental Modelling & Software*, 26(6):804–816, June 2011.

[51] DNDC - Scientific Basis and Processes. Technical report, University of New Hampshire, June 2017.

[52] Kerry A. Nice, Andrew M. Coutts, and Nigel J. Tapper. Development of the VTUF-3D v1.0 urban micro-climate model to support assessment of urban vegetation influences on human thermal comfort. *Urban Climate*, 24:1052–1076, June 2018. 11.

[53] ENVI-met Model Architecture [A holistic microclimate model].

[54] Wanlu Ouyang, Tim Sinsel, Helge Simon, Tobi Eniolu Morakinyo, Huimin Liu, and Edward Ng. Evaluating the thermal-radiative performance of ENVI-met model for green infrastructure typologies: Experience from a subtropical climate. *Building and Environment*, 207:108427, January 2022.

[55] World Bank. Climate change knowledge portal. `https://climateknowledgeportal.worldbank.org/country/netherlands`. Accessed: August 16, 2023.

[56] Stephan van Eps. Thermische gedragsanalyse van verschillende grondsystemen boven een permavoid laag. Technical report, Technical University Delft, 2023.

[57] Yuhan Mao. *Changing patterns of thermal behaviour of concrete pavements in diurnal periods*. Additional Thesis, TU Delft, 2022.

[58] The Concrete Centre. Surface emmissivity - why this matters. `https://www.concretecentre.com/Performance-Sustainability/Thermal-Mass/Surface-emissivity-why-this-matters.aspx#:~:text=This%20basically%20relates%20to%20how%20shiny%20or%20matt,very%20good%20at%20absorbing%20and%20emitting%20radiant%20heat.` Accessed: August 16, 2023.

[59] material properties. Concrete – density – heat capacity – thermal conductivity. `https://material-properties.org/concrete-density-heat-capacity-thermal-conductivity/`. Accessed: August 16, 2023.

[60] Martin Venturas, Rosana López, Antonio Gascó, and Luis Gil. Hydraulic properties of european elms: xylem safety-efficiency tradeoff and species distribution in the iberian peninsula. *Trees*, 27:1691–1701, 2013.

[61] Blandine Caquet, Têtè S Barigah, Hervé Cochard, Pierre Montpied, Catherine Collet, Erwin Dreyer, and Daniel Epron. Hydraulic properties of naturally regenerated beech saplings respond to canopy opening. *Tree physiology*, 29(11):1395–1405, 2009.

[62] A Rzepecki, F Zeng, and FM Thomas. Xylem anatomy and hydraulic conductivity of three co-occurring desert phreatophytes. *Journal of Arid Environments*, 75(4):338–345, 2011.

[63] R. A. Duursma and B. E. Medlyn. MAESPA: a model to study interactions between water limitation, environmental drivers and vegetation function at tree and stand levels, with an example application to [CO₂] × drought interactions. *Geoscientific Model Development*, 5(4):919–940, July 2012. 11 linked.

[64] B. E. Medlyn, D. A. Pepper, A. P. O'Grady, and H. Keith. Linking leaf and tree water use with an individual-tree model. *Tree Physiology*, 27(12):1687–1699, December 2007.

[65] M. Williams, B. J. Bond, and M. G. Ryan. Evaluating different soil and plant hydraulic constraints on tree function using a model and sap flow data from ponderosa pine: Soil and plant hydraulics. *Plant, Cell & Environment*, 24(7):679–690, July 2001.

[66] M. Williams, B. E. Law, P. M. Anthoni, and M. H. Unsworth. Use of a simulation model and ecosystem flux data to examine carbon-water interactions in ponderosa pine. *Tree Physiology*, 21(5):287–298, March 2001.

[67] Kerry Nice. Vtuf-3d code repository: Vtuf-3d initial release [data set]. `http://dx.doi.org/10.5281/zenodo.260064`, 2017.

[68] Botanic Gardens of South Australia. Plant selector. `http://plantselector.botanicgardens.sa.gov.au/Plants/Details/141`. Accessed: August 16, 2023.

[69] iplantz - usefull plants for warm climates. `https://www.iplantz.com/plant/979/lophostemon-confertus/`. Accessed: August 16, 2023.

[70] Cabi digital library. `https://www.cabidigitallibrary.org/doi/10.1079/cabicompendium.23983#sec-33`. Accessed: August 16, 2023.

[71] Peter Broede, Krzysztof Blazejczyk, Dusan Fiala, George Havenith, Ingvar Holmer, Gerd Jendritzky, Kalev Kuklane, and Bernhard Kampmann. The universal thermal climate index utci compared to ergonomics standards for assessing the thermal environment. *Industrial health*, 51(1):16–24, 2013.